

International Atomic Energy Agency

INDC(CCP)-369

Distr.: L

INDC

INTERNATIONAL NUCLEAR DATA COMMITTEE

**SECONDARY NEUTRON EMISSION SPECTRA FROM
SPHERICAL AND HEMISPHERICAL SAMPLES OF MATERIALS
OBTAINED AT 14 MeV NEUTRON ENERGY**

A.I. Saukov, B.I. Sukhanov, A.M. Ryabinin
All-Union Scientific Research Institute of Engineering Physics
Chelyabinsk, Russian Federation

(Translated from a Russian original published in Yadernye Konstanty 4/1991)

Translation editor: Dr. A. Lorenz

February 1994

IAEA NUCLEAR DATA SECTION, WAGRAMERSTRASSE 5, A-1400 VIENNA

Reproduced by the IAEA in Austria
February 1994

SECONDARY NEUTRON EMISSION SPECTRA
FROM SPHERICAL AND HEMISPHERICAL SAMPLES OF MATERIALS
OBTAINED AT 14 MEV NEUTRON ENERGY

A.I. Saukov, B.I. Sukhanov, A.M. Ryabinin
All-Union Scientific Research Institute of
Engineering Physics, Chelyabinsk

ABSTRACT

Results of secondary neutron spectra measurements carried out in the 0.4-14 MeV energy range on spherical and hemispherical samples of Mg, Al, Fe, Ni, Cu, Zr, Ti, Mo, C, CF, Pb, ^{238}U , Be, H_2O , D_2O and CH_2 using the time-of-flight method at 14 MeV neutron energy are presented. The experimental results are given in the form of normalized measured emission spectra for 13 neutron energy ranges. The results obtained can be used to improve the quality of existing nuclear data libraries.

In recent years there has been an increased interest in integral experiments to verify entire sets of neutron data for a given element [1]. In view of this we carried out a series of experiments to measure neutron spectra emitted from spherical and hemispherical samples of various construction elements and materials bombarded with 14 MeV neutrons. The materials investigated were: Mg, Al, Fe, Ti, Ni, Cu, Zr, Mo, CF_2 , Pb, ^{238}U , H_2O , D_2O , Be, C and CH_2 . In our opinion the results obtained from the hemispherical samples (inverse hemispheres) are particularly interesting as they enable verification of neutron elastic and inelastic scattering cross-sections at large angles, which are difficult to measure on small samples, and are, as a rule, inaccurate.

The measurements were carried out using the time-of-flight method with a flight path of 8.5 m using a detector with a 70 x 70 mm stilbene crystal and an FEU-110 (photomultiplier) with neutron-gamma separation to reduce the gamma-ray background. The

neutron detection threshold was 0.15 MeV. The pulsed neutron generator parameters were as follows:

Neutron pulse duration (width):	15 nsec
Pulse frequency:	500 kHz
Mean neutron yield:	3.10^8 neutrons/sec

In order to reduce the flux of direct 14 MeV neutrons, and also to obtain more precise information on the magnitude of 14 MeV neutron elastic scattering on the samples, a steel rod 30, mm in diameter and 400 mm in length, was placed between the target and the detector such that it completely covered the 25 mm diameter target with the result that it had a weak effect on the neutron flux scattered by the sample. The sample data are given in Table 1 and the experimental set-up is shown in Fig. 1.

All experimental results are normalized to 1000 14 MeV neutrons recorded by the detector with no shielding rod.

Based on numerous experiments and calculations, the detector efficiency was derived by comparing the experimental and calculated spectra of a spherical sample of ^{238}U . (Calculations of ^{238}U , CH_2 and Pb spectra have been carried out in Refs [2, 3] using the Monte Carlo method.) The relative detector efficiencies used in our experiments are given in Table 2. In order to provide additional data and enhance the accuracy of the energy dependence of the efficiency, independent measurements were made at 1.48 and 2.64 MeV, using a polyethylene ring-shaped scatterer. The results of these measurements, which were based on the well-known 14.5 MeV elastic scattering cross-section for hydrogen, agreed with the accepted efficiency value to within $\pm 4\%$. A further corroboration of the detector efficiency used is the good agreement between calculated and experimental spectra of such well-studied materials as polyethylene and lead. On the whole, we consider that the detector efficiency we used is accurate to within $\pm 5\%$.

We should add that in basing our measurements on the ^{238}U spectrum we exclude errors attributable to changes in the experimental set-up, shifts in detection thresholds, replacement of and damage to the detector crystals. This approach to determining detector efficiency means that our results can be reproduced in other laboratories. Should our standard ^{238}U neutron spectrum differ somewhat from the real spectrum, corresponding corrections can be made by measuring other samples.

The accepted detector efficiency allows for neutron scattering in air (for a flight path of 8.5 m) and scattering from materials surrounding the detector (packing of the crystal, photomultiplier, detector housing and protection). Since all these effects have to some extent a resonance character (particularly scattering in air), the detector efficiency should, strictly speaking, reflect this resonance structure. As this structure does not exceed 4-5% in most of the spectrum in our energy resolution, we felt we could retain a smooth efficiency character, except for the 920 nsec region (neutron energy $E_n = 0.44$ MeV) where strong resonance in oxygen leads to a drop of up to 15% in the efficiency curve.

All the measurement results are given in the form of measured spectra $\Delta N/\Delta t$ as a function of neutron flight time at time intervals $\Delta t = 10^{-8}$ sec. This way of presenting data has specific advantages compared to the traditional form of energy dependence: $\Delta n/\Delta E = f(E_n)$. For normal co-ordinates the neutron spectrum tends to infinity as neutron energy tends to zero. The measurement error increases sharply as the neutron energy approaches the detection threshold. Furthermore, at high energies ($E_n > 8$ MeV) the energy resolution capability of the time-of-flight method decreases sharply, approaching ± 1.2 MeV in the 14 MeV region, while for a neutron energy of 0.5 MeV the resolution is 0.022 MeV.

In the light of this, the neutron spectrum graph using normal co-ordinates is quite unsuitable for analyses purposes

since much of the figure contains useless data, with a large error, and the main part of the spectrum is depicted on a small scale and is concentrated in one tiny area. On the contrary, the measured spectrum shown as a function of flight time has a more or less even error distribution both for time and amplitude over the whole region of the figure.

The statistical accuracy of the experiments in the 1-3 MeV region, where the main neutron group is concentrated, did not exceed +2%. We consider the total accuracy in this region to be +5%. The measurement results are given in Figs 2-33, and all of the data are normalized to 1000 14 MeV neutrons.

Before going on to discussion of the results let us take a look at Fig. 34 which shows the ^{238}U spectrum after passing through a 2 cm layer of Be. This spectrum, represented in relative units, is mainly used as for energy calibration of the time-of-flight spectrometer. The marked dip at 780 nsec (0.62 MeV) shows good agreement with the clearly expressed resonance in the total beryllium cross-section. Besides its primary function, this figure also illustrates the fact that time resolution of the method used is more or less independent of the time-of-flight since the natural width of the beryllium resonance did not increase in our measurements.

Integral experiments on spherical samples obtained at 14 MeV have also been carried out at other laboratories: reference [4] describes measurements on carbon, oxygen, aluminum, titanium and iron; reference [5] measurements of spectra emitted by a water sphere; references [6, 7] spectra from iron spheres; reference [8, 9] spectra from lead; and references [10, 11] spectra from uranium-238 and beryllium.

Unfortunately, it is difficult to make a direct comparison of the data obtained in the various laboratories as the experiments were carried out under diverse conditions and with samples of different dimensions. The results obtained by

different authors can therefore only be compared through appropriate calculations using certain nuclear data. Although each of the above papers provides some comparisons of calculations carried out at the same laboratory, there is no comparison with experiments performed at other laboratories, so that possible errors in experiment and calculation remain undetected. Reference [3] provides partial comparison of experimental data from various authors for ^{238}U , CH_2 and Pb . This should be extended to other elements and materials.

We should also point out that the published data is of limited usefulness. For example, Ref. [4] which deals with emission spectra from C, O, Al, Fe and Ti includes only data for neutron energies greater than 2 MeV. As a result we cannot verify the elemental neutron data for inelastically scattered neutrons which lie below 2 MeV. As a rule, the data are presented in the form of a logarithmic graph with no numerical figures which makes comparison of results difficult.

It would be desirable to come to some agreement with other laboratories, performing such measurements, on standardized sample dimensions and data presentation as has been done for standard measurements of reference neutron cross-sections, in order to attain a good degree of accuracy when comparing experimental data with nuclear data libraries.

Table 1
Sample parameters

No.	Sample	Mass of hemisphere, kg	Mass of sphere, Kg	Sample dimensions, mm
1	Mg	3,260	6,590	200x100
2	Al	4,880	9,860	200x100
3	Fe	13,330	26,900	198x99
4	Ti	7,920	16,170	200x100
5	Ni	14,820	29,910	200x100
6	Cu	14,750	29,920	197x100
7	Zr ^{*)}	11,710	23,660	200x98
8	Mo ^{*)}	17,810	36,070	200x100
9	CF ₂	3,900	7,860	200x100
10	Pb	19,250	39,110	200x100
11	²³⁸ U	33,300	67,800	200x100
12	H ₂ O	1,780	3,600	200x100
13	D ₂ O	1,96	3,95	200x100
14	Be	6,300	12,670	260x160
15	C	2,215	4,550	180x100
16	CH ₂	1,620	3,280	200x100

[*] As these samples were made of sheet material, their average densities may vary somewhat from the normal value.

Table 2
Detector efficiency

Time,nsec	ϵ , rel.	Time,nsec	ϵ ,rel.	Time,nsec	ϵ , rel.
100	1,0	40	1,47	80	1,71
20	1,0	60	1,50	800	1,73
40	1,0	80	1,52	20	1,75
60	1,0	500	1,54	40	1,76
80	1,0	20	1,55	60	1,73
200	1,02	40	1,56	80	1,65
20	1,04	60	1,56	900	1,56
40	1,08	80	1,57	20	1,50
60	1,12	600	1,58	40	1,50
80	1,17	20	1,59	60	1,52
300	1,22	40	1,61	80	1,55
20	1,26	60	1,64	1000	1,53
40	1,31	80	1,67	20	1,50
60	1,35	700	1,68	40	1,45
80	1,39	20	1,69	60	1,40
400	1,42	40	1,69	80	-
20	1,44	60	1,70	1100	-

CAPTIONS

- Fig. 1. Experimental set-up. 1: sample to be measured, 2: Pulsed neutron beam monitors, 3: Polyethylene collimator, 4: All-frequency counters, 5: Collimator-lead, 6: Detector shield-lead, 7: Detector, 8: Collimator-polyethylene, 9: Concrete wall, 10: Steel rod, 11: 14 MeV neutron source.
- Fig. 2. Normalized measured spectrum of hemispherical sample of magnesium.
- Fig. 3. Normalized measured spectrum of spherical sample of magnesium.
- Fig. 4. Normalized measured spectrum of hemispherical sample of aluminum.
- Fig. 5. Normalized measured spectrum of spherical sample of aluminum.
- Fig. 6. Normalized measured spectrum of hemispherical sample of iron.
- Fig. 7. Normalized measured spectrum of spherical sample of iron.
- Fig. 8. Normalized measured spectrum of hemispherical sample of titanium.
- Fig. 9. Normalized measured spectrum of spherical sample of titanium.
- Fig. 10. Normalized measured spectrum of hemispherical sample of nickel.
- Fig. 11. Normalized measured spectrum of spherical sample of nickel.
- Fig. 12. Normalized measured spectrum of hemispherical sample of copper.
- Fig. 13. Normalized measured spectrum of spherical sample of copper.
- Fig. 14. Normalized measured spectrum of hemispherical sample of zirconium.
- Fig. 15. Normalized measured spectrum of spherical sample of zirconium.
- Fig. 16. Normalized measured spectrum of hemispherical sample of molybdenum.

- Fig. 17. Normalized measured spectrum of spherical sample of molybdenum.
- Fig. 18. Normalized measured spectrum of hemispherical sample of fluoroplastic.
- Fig. 19. Normalized measured spectrum of spherical sample of fluoroplastic.
- Fig. 20. Normalized measured spectrum of hemispherical sample of lead.
- Fig. 21. Normalized measured spectrum of spherical sample of lead.
- Fig. 22. Normalized measured spectrum of hemispherical sample of ^{238}U .
- Fig. 23. Normalized measured spectrum of spherical sample of ^{238}U .
- Fig. 24. Normalized measured spectrum of hemispherical sample of water
- Fig. 25. Normalized measured spectrum of spherical sample of water.
- Fig. 26. Normalized measured spectrum of hemispherical sample of heavy water.
- Fig. 27. Normalized measured spectrum of spherical sample of heavy water.
- Fig. 28. Normalized measured spectrum of hemispherical sample of beryllium.
- Fig. 29. Normalized measured spectrum of spherical sample of beryllium.
- Fig. 30. Normalized measured spectrum of hemispherical sample of carbon.
- Fig. 31. Normalized measured spectrum of spherical sample of carbon.
- Fig. 32. Normalized measured spectrum of hemispherical sample of polyethylene.
- Fig. 33. Normalized measured spectrum of spherical sample of polyethylene.
- Fig. 34. Measured spectrum of hemispherical sample of ^{238}U which has passed through a 2 cm layer of beryllium.

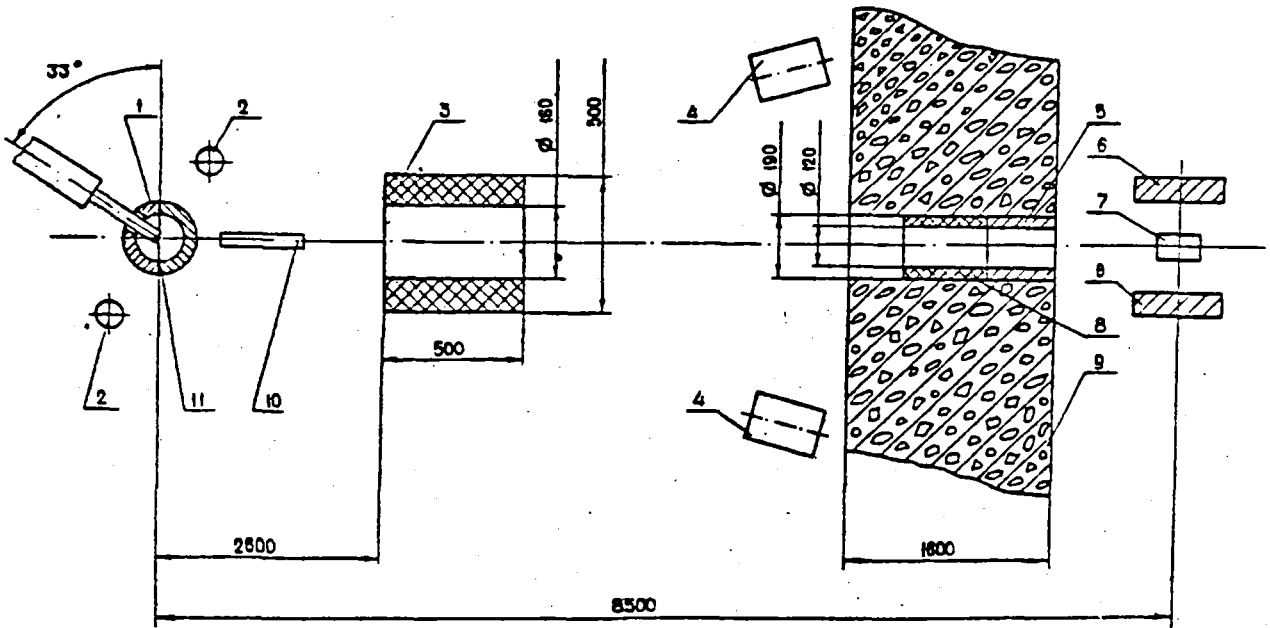


Fig. 1. Experimental set-up. 1: sample to be measured, 2: Pulsed neutron beam monitors, 3: Polyethylene collimator, 4: All-frequency counters, 5: Collimator-lead, 6: Detector shield-lead, 7: Detector, 8: Collimator-polyethylene, 9: Concrete wall, 10: Steel rod, 11: 14 MeV neutron source.

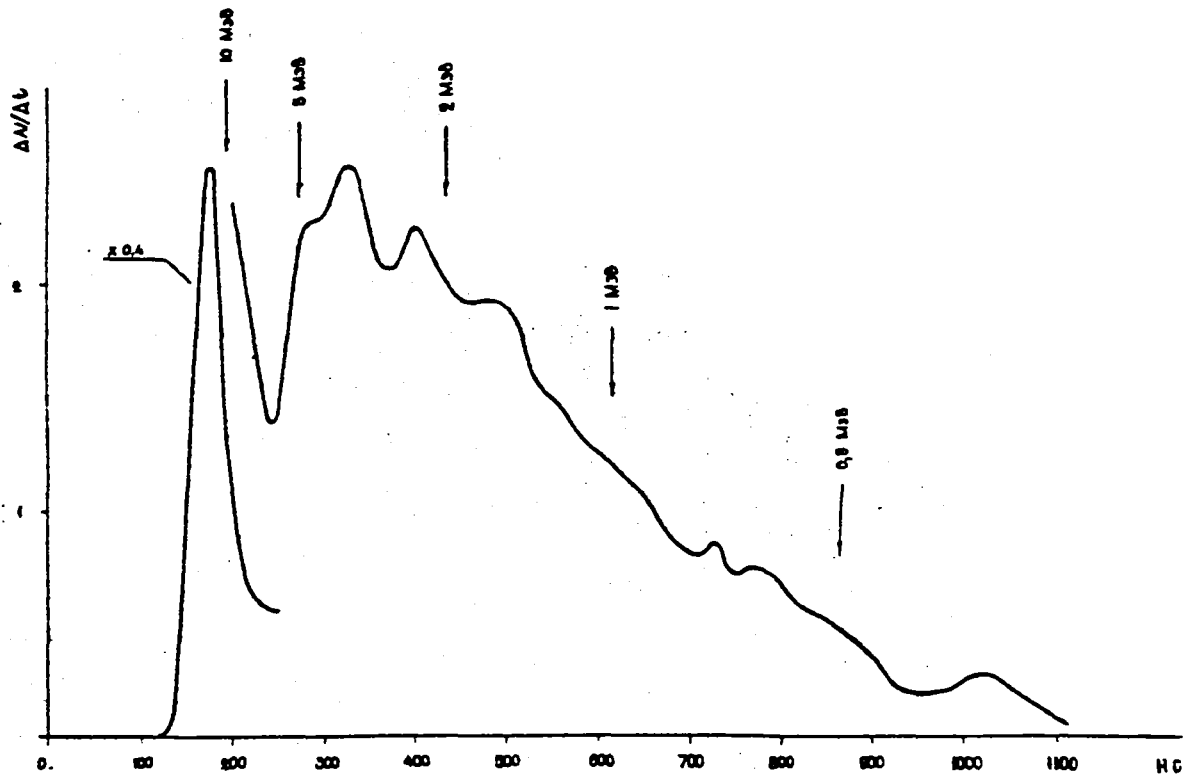


Fig. 2. Normalized measured spectrum of hemispherical sample of magnesium.

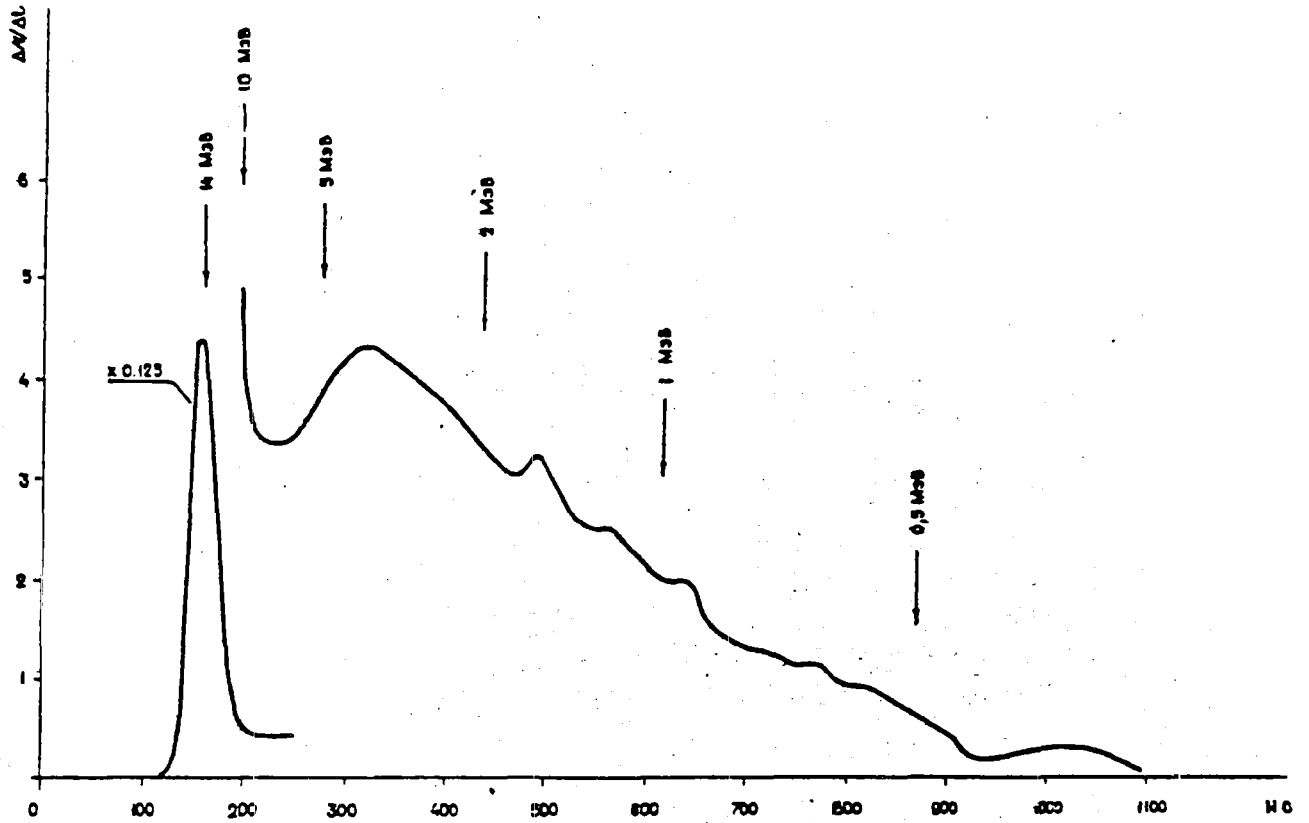


Fig. 3. Normalized measured spectrum of spherical sample of magnesium.

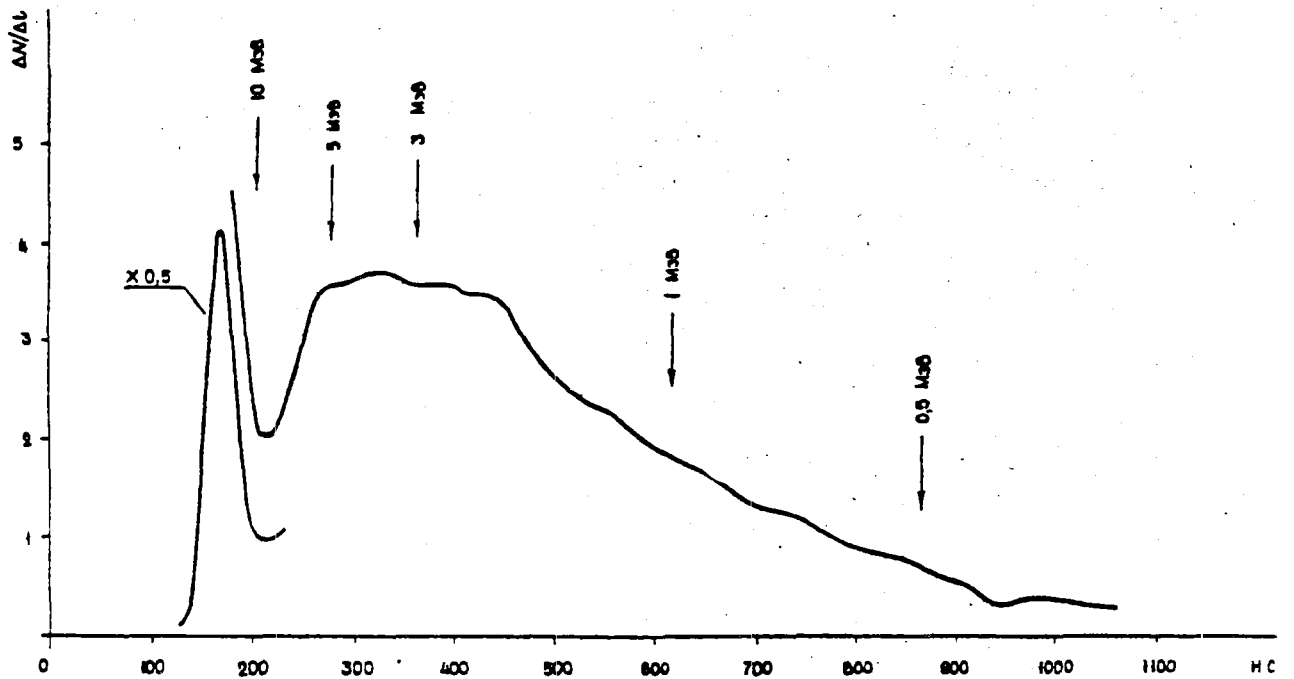


Fig. 4. Normalized measured spectrum of hemispherical sample of aluminum.

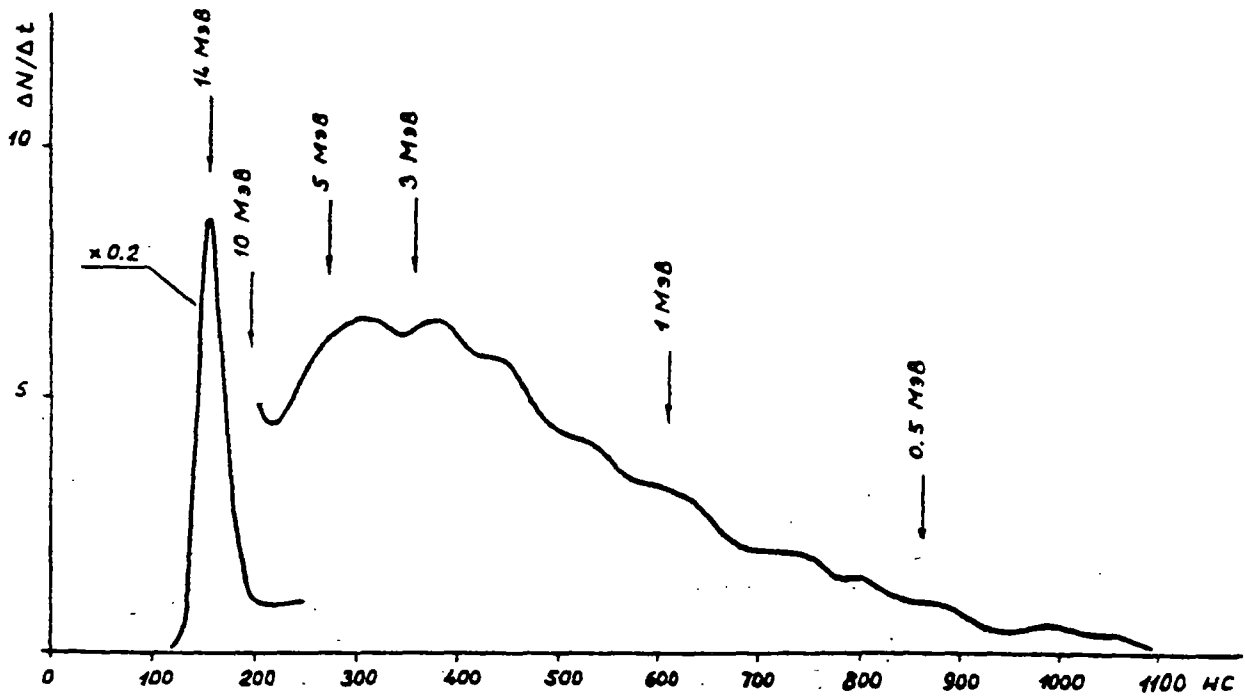


Fig. 5. Normalized measured spectrum of spherical sample of aluminum.

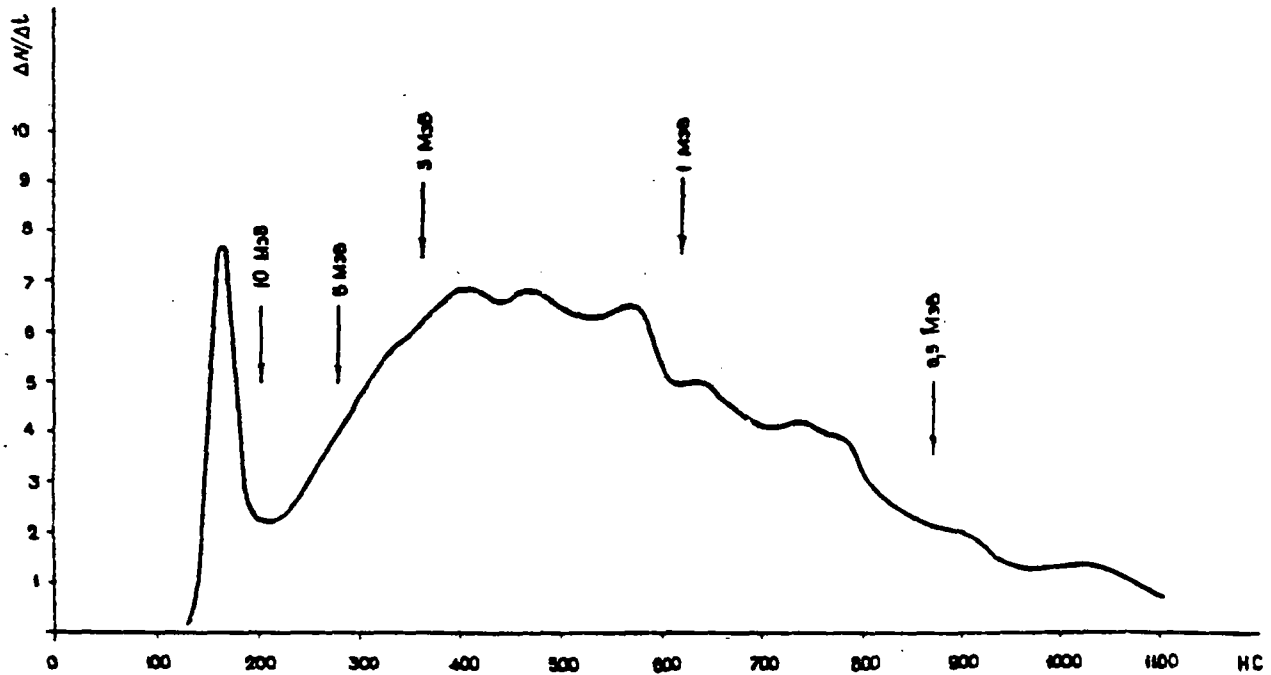


Fig. 6. Normalized measured spectrum of hemispherical sample of iron.

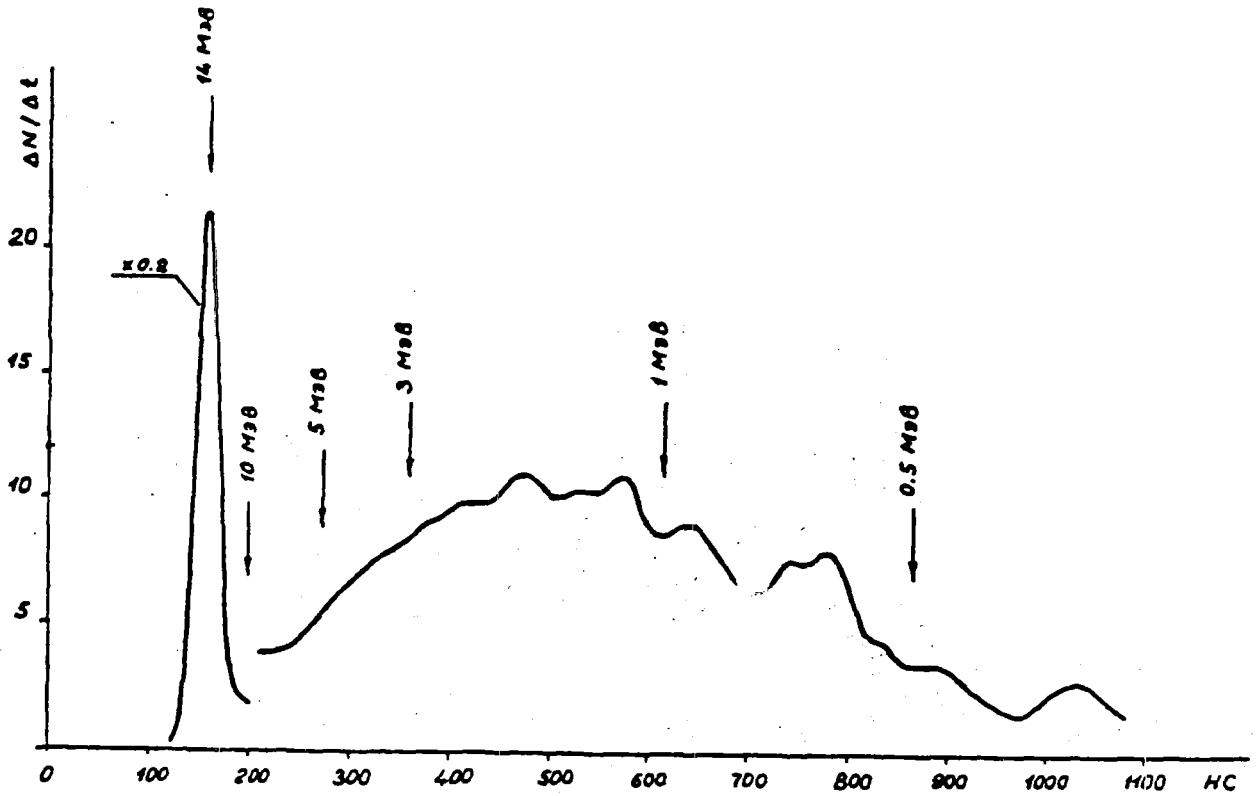


Fig. 7. Normalized measured spectrum of spherical sample of iron.

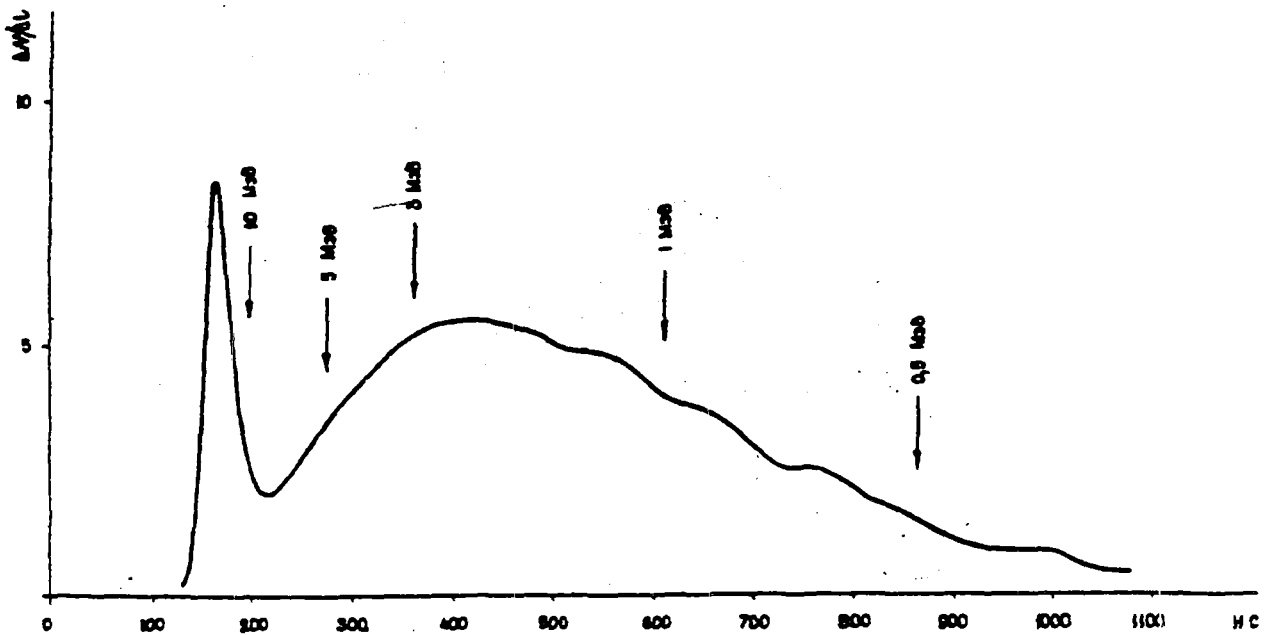


Fig. 8. Normalized measured spectrum of hemispherical sample of titanium.

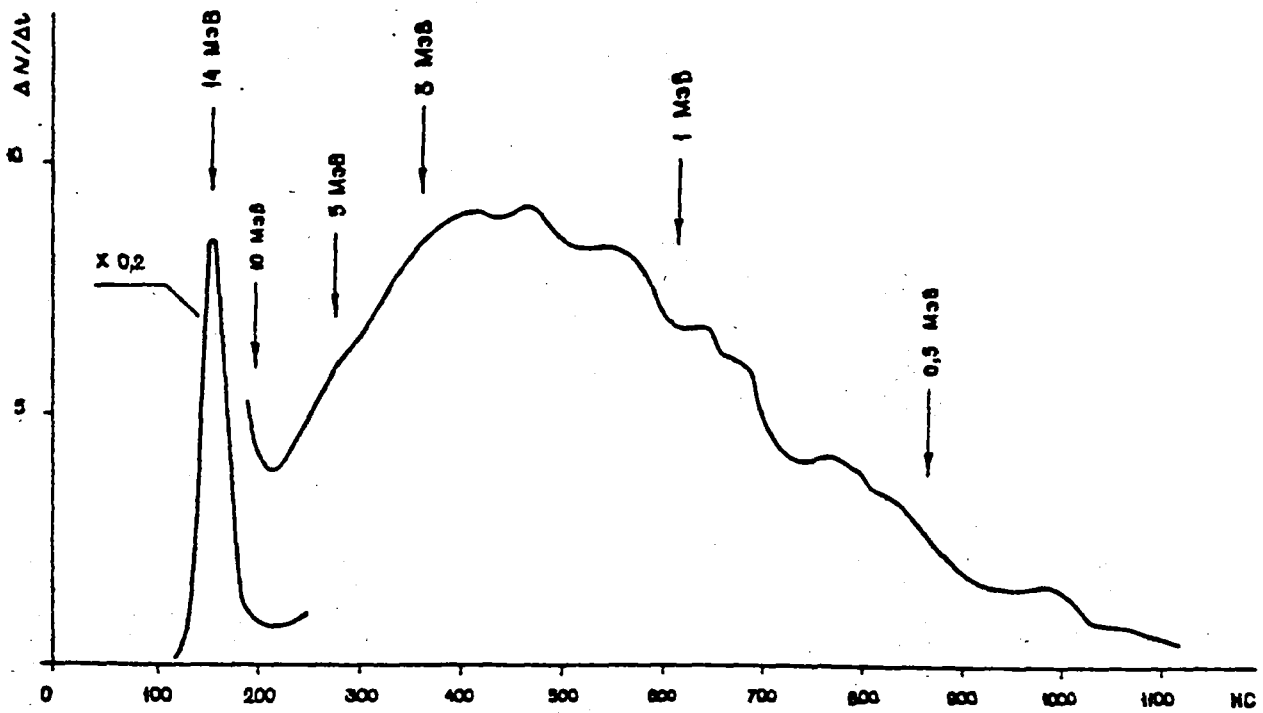


Fig. 9. Normalized measured spectrum of spherical sample of titanium.

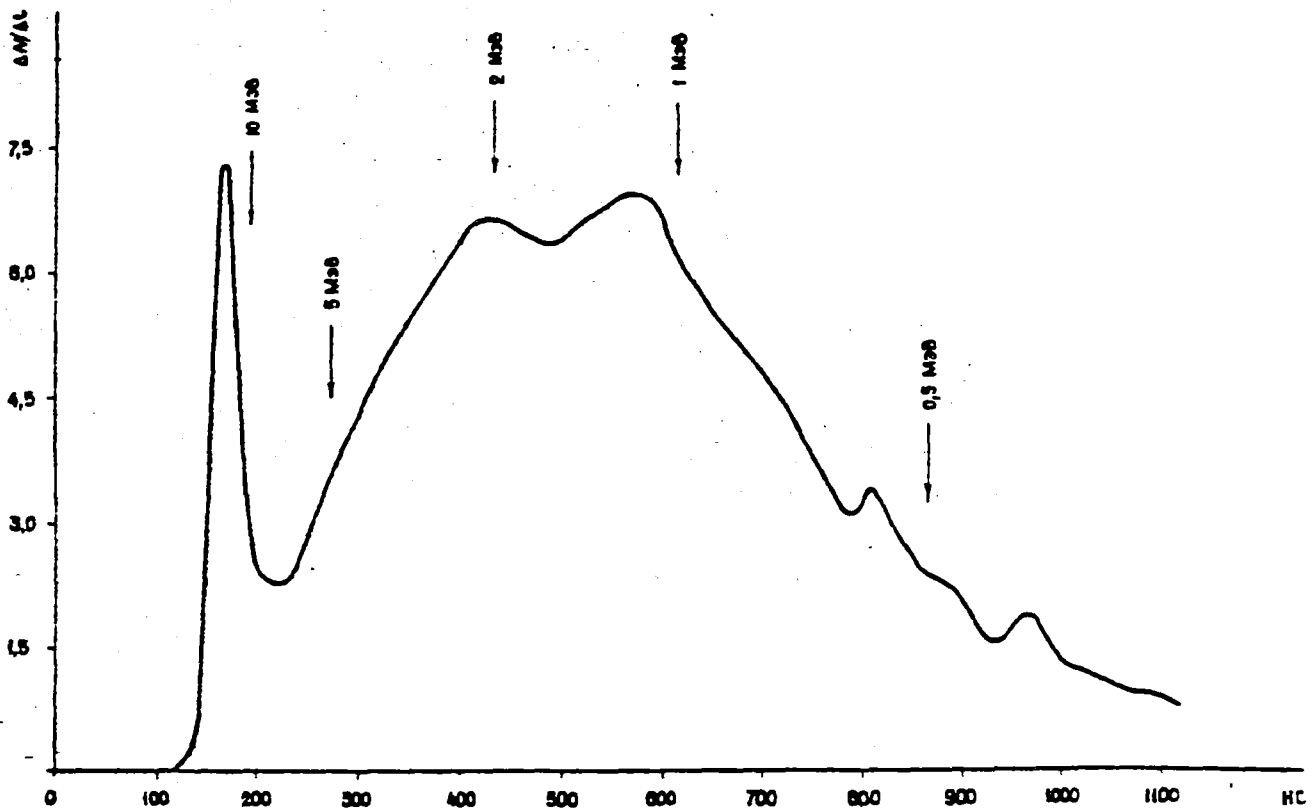


Fig. 10. Normalized measured spectrum of hemispherical sample of nickel.

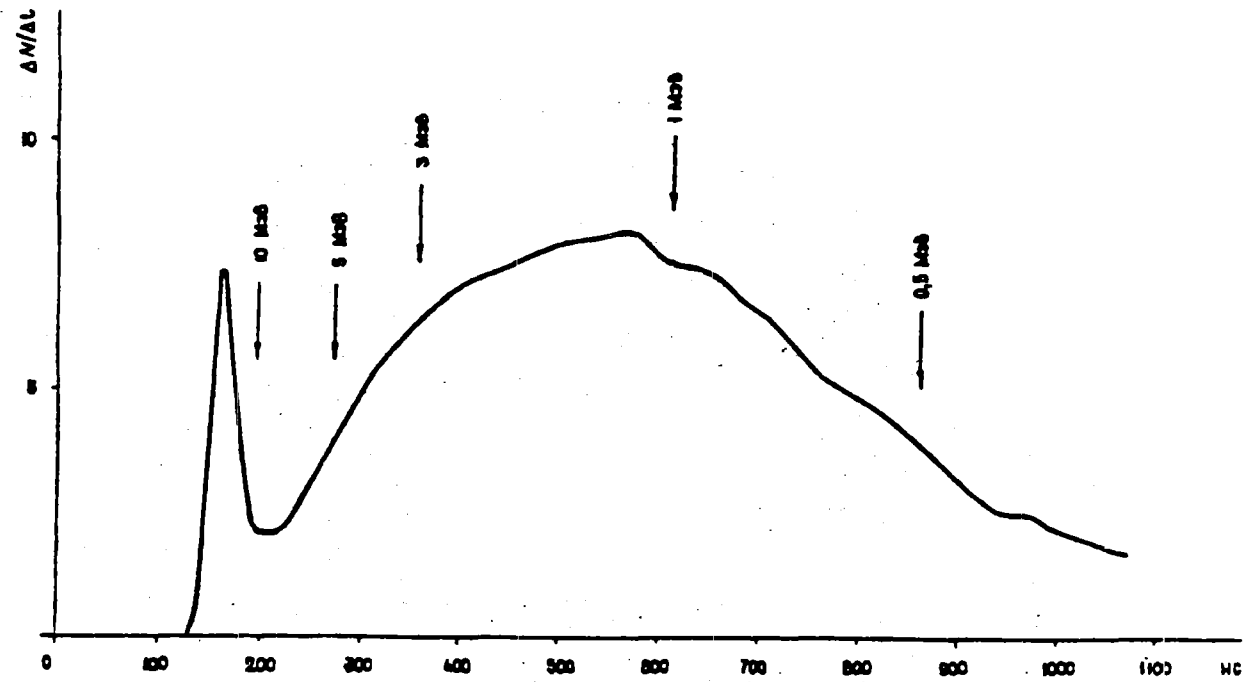


Fig. 11. Normalized measured spectrum of spherical sample of nickel.

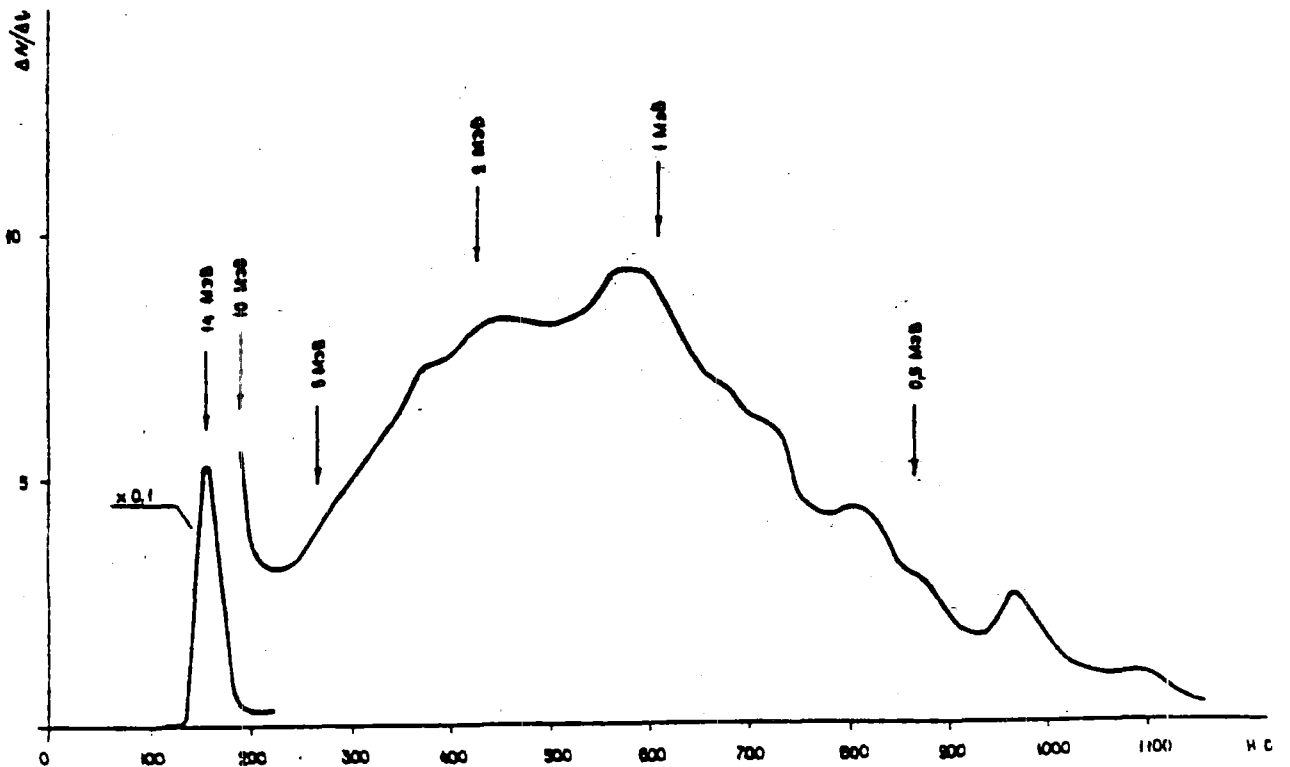


Fig. 12. Normalized measured spectrum of hemispherical sample of copper.

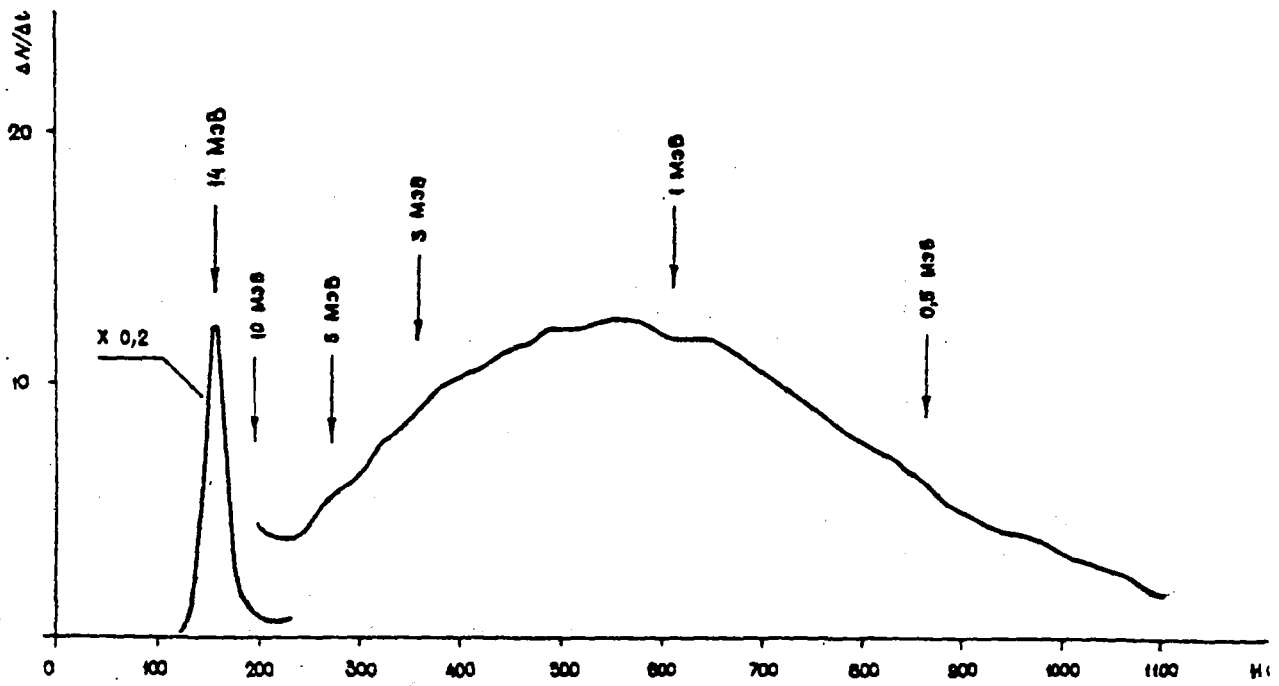


Fig. 13. Normalized measured spectrum of spherical sample of copper.

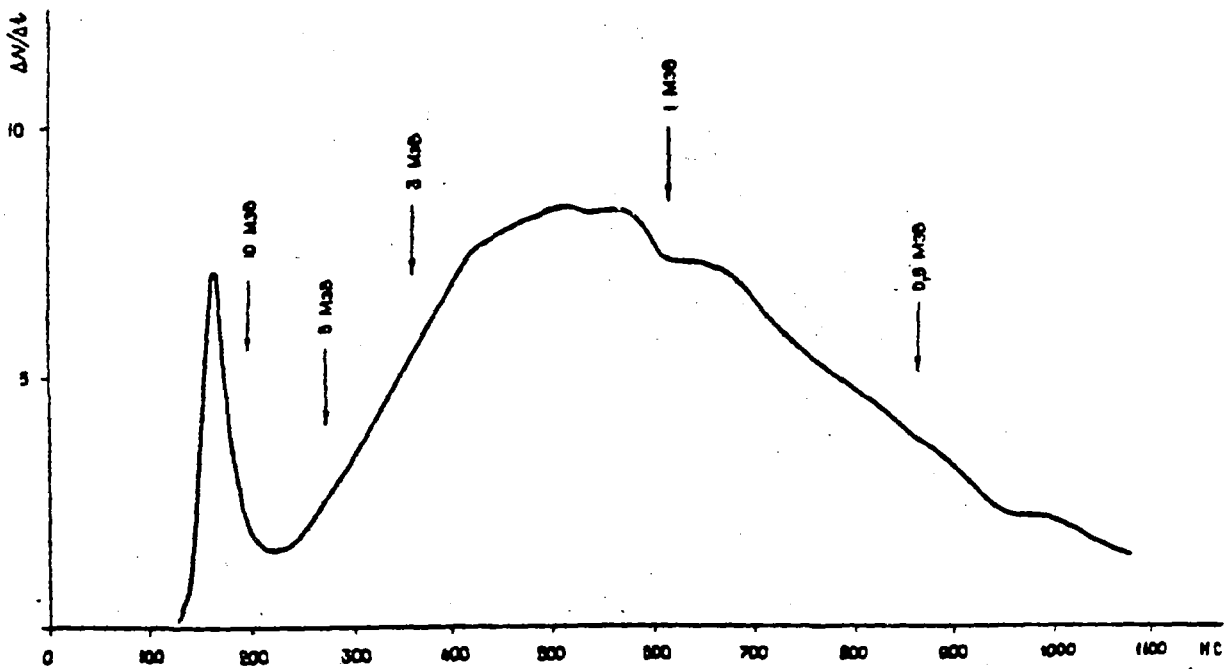


Fig. 14. Normalized measured spectrum of hemispherical sample of zirconium.

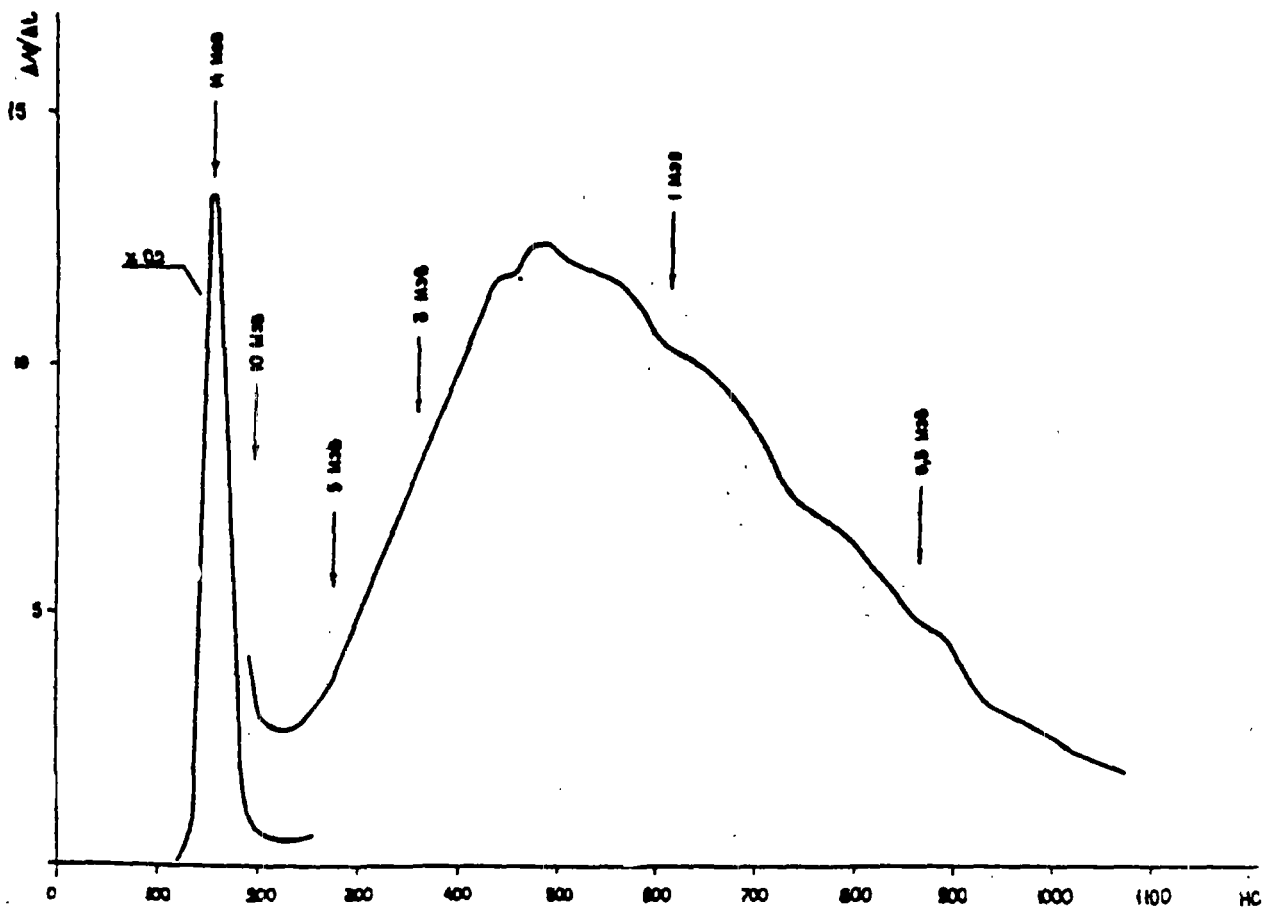


Fig. 15. Normalized measured spectrum of spherical sample of zirconium.

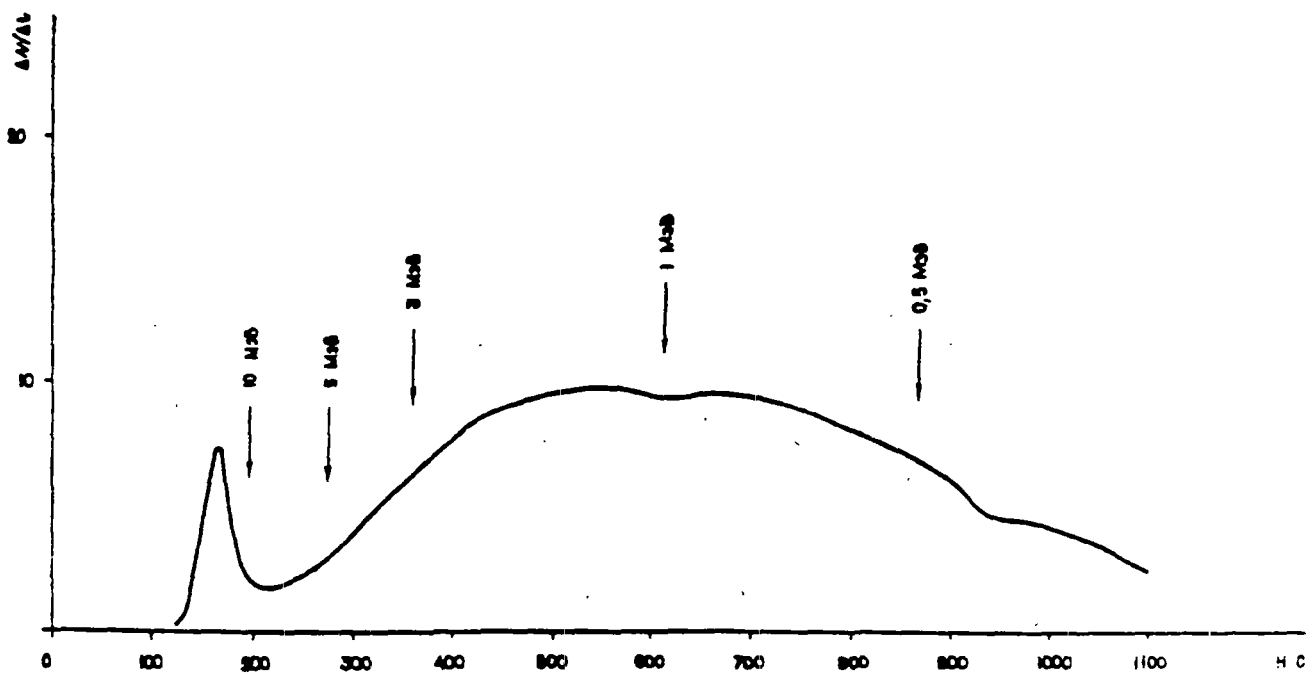


Fig. 16. Normalized measured spectrum of hemispherical sample of molybdenum.

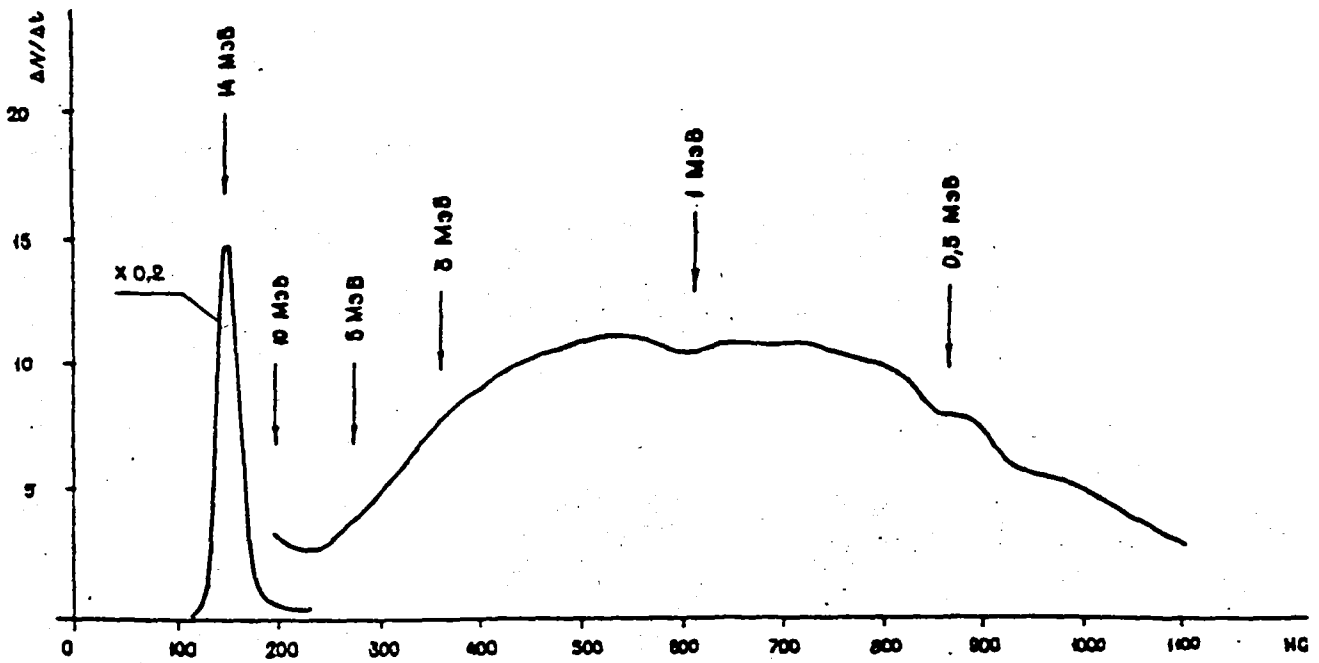


Fig. 17. Normalized measured spectrum of spherical sample of molybdenum.

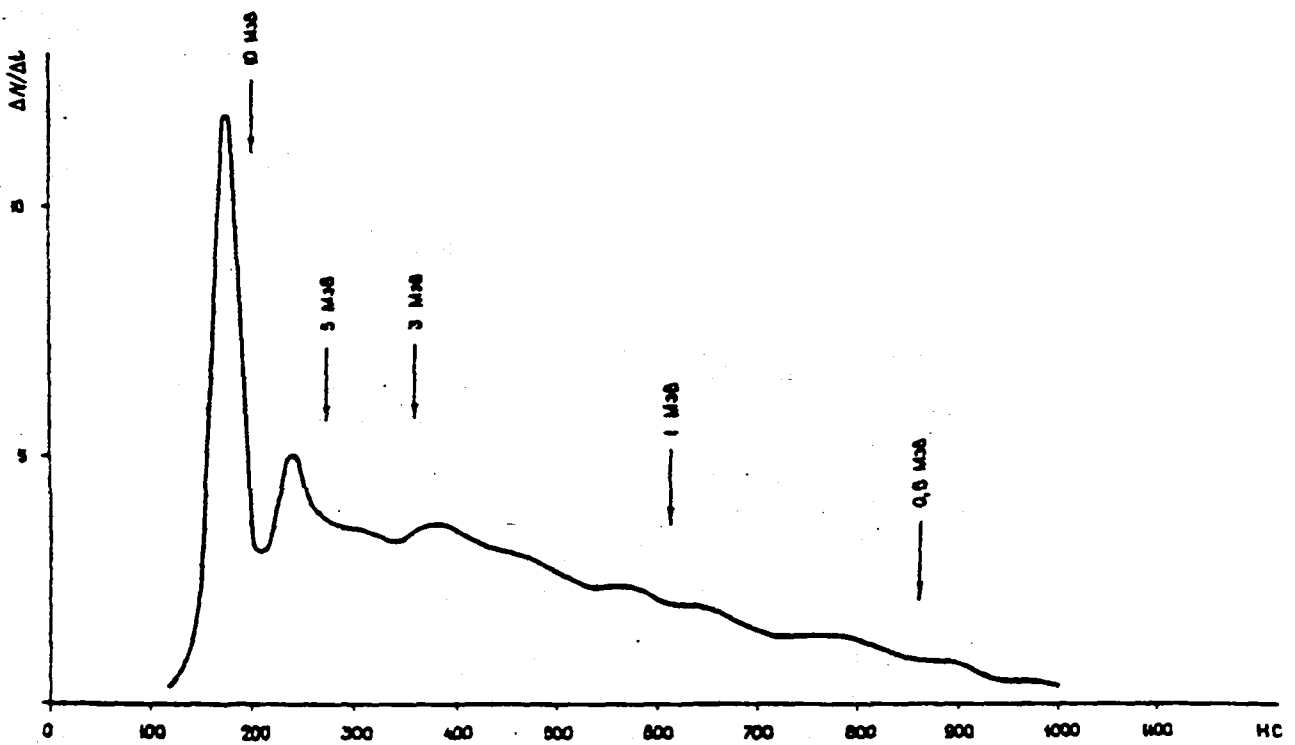


Fig. 18. Normalized measured spectrum of hemispherical sample of fluoroplastic.

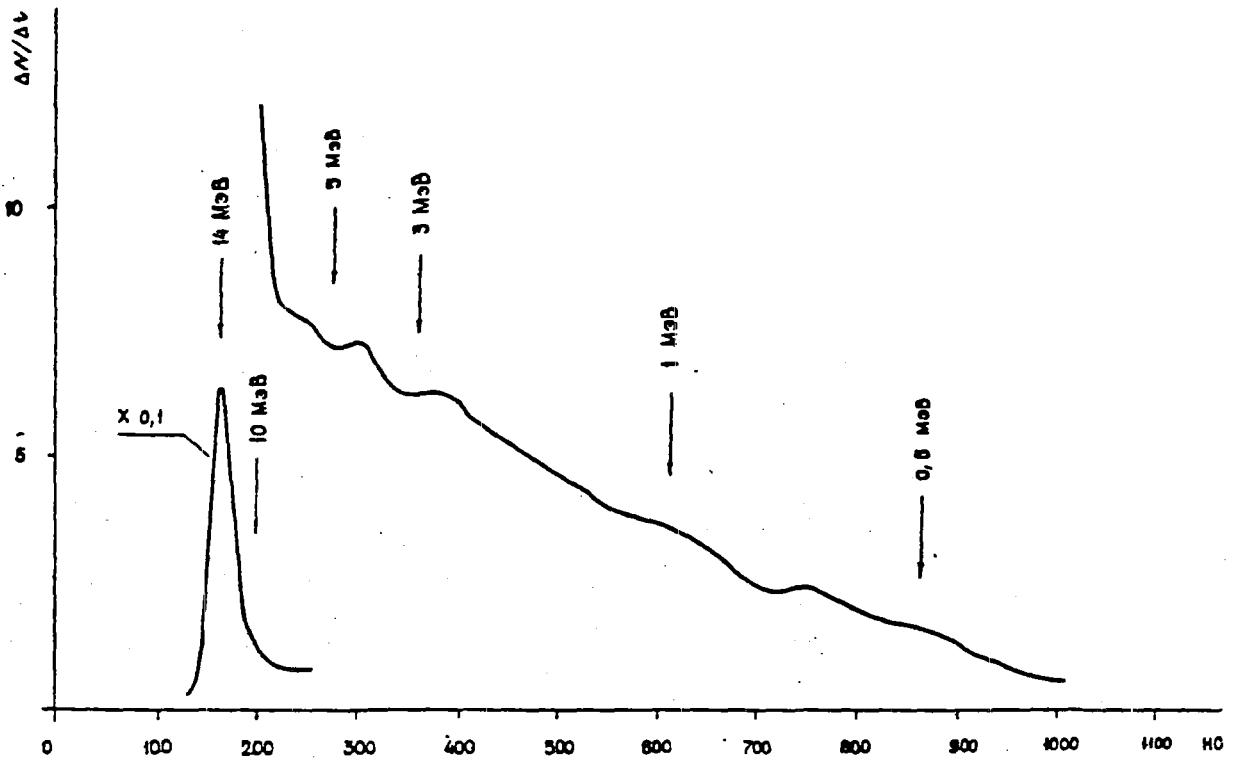


Fig. 19. Normalized measured spectrum of spherical sample of fluoroplastic.

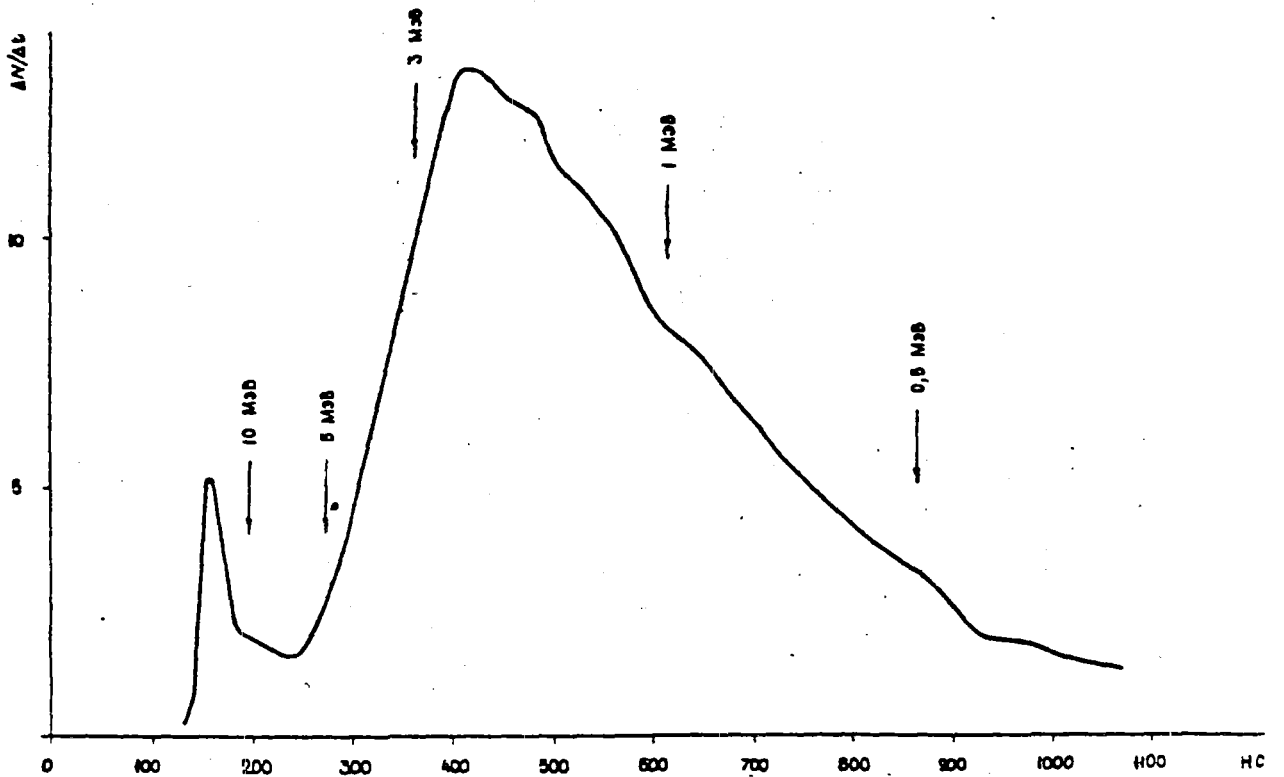


Fig. 20. Normalized measured spectrum of hemispherical sample of lead.

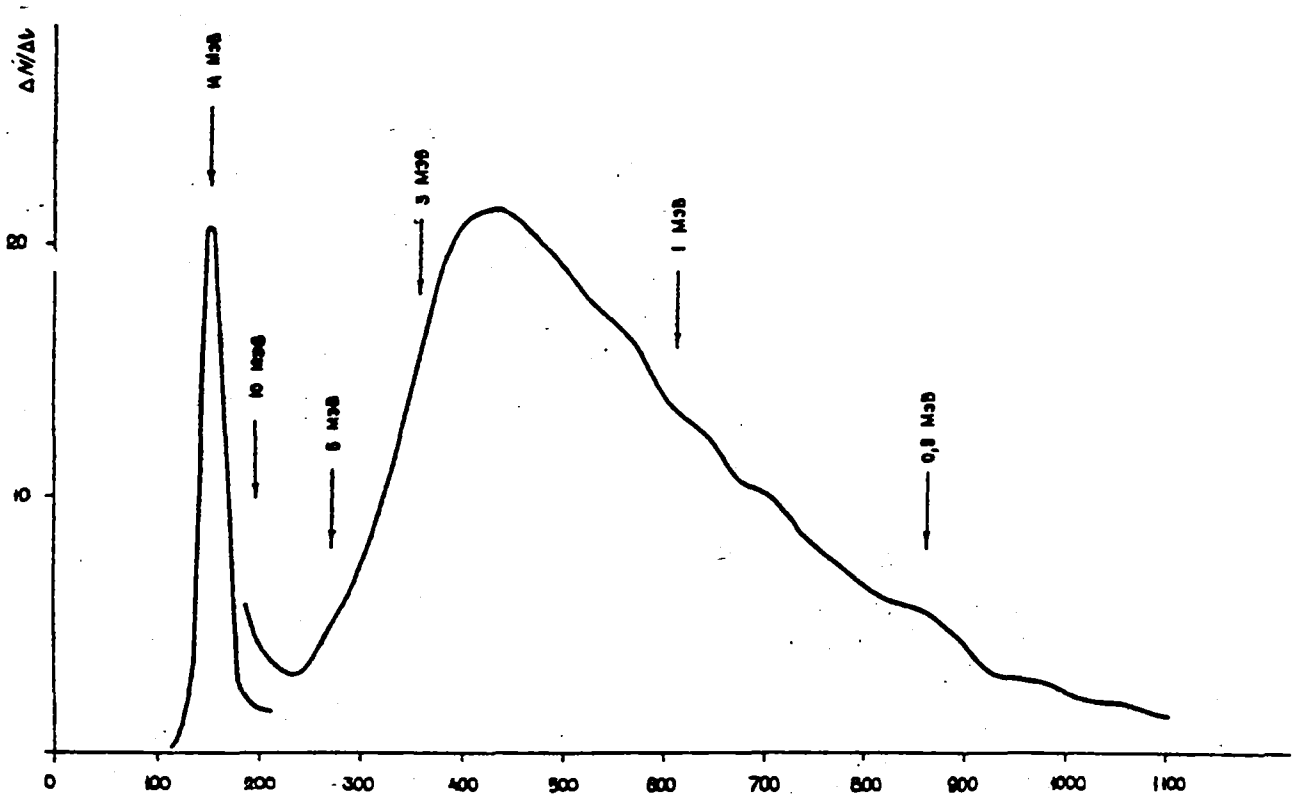


Fig. 21. Normalized measured spectrum of spherical sample of lead.

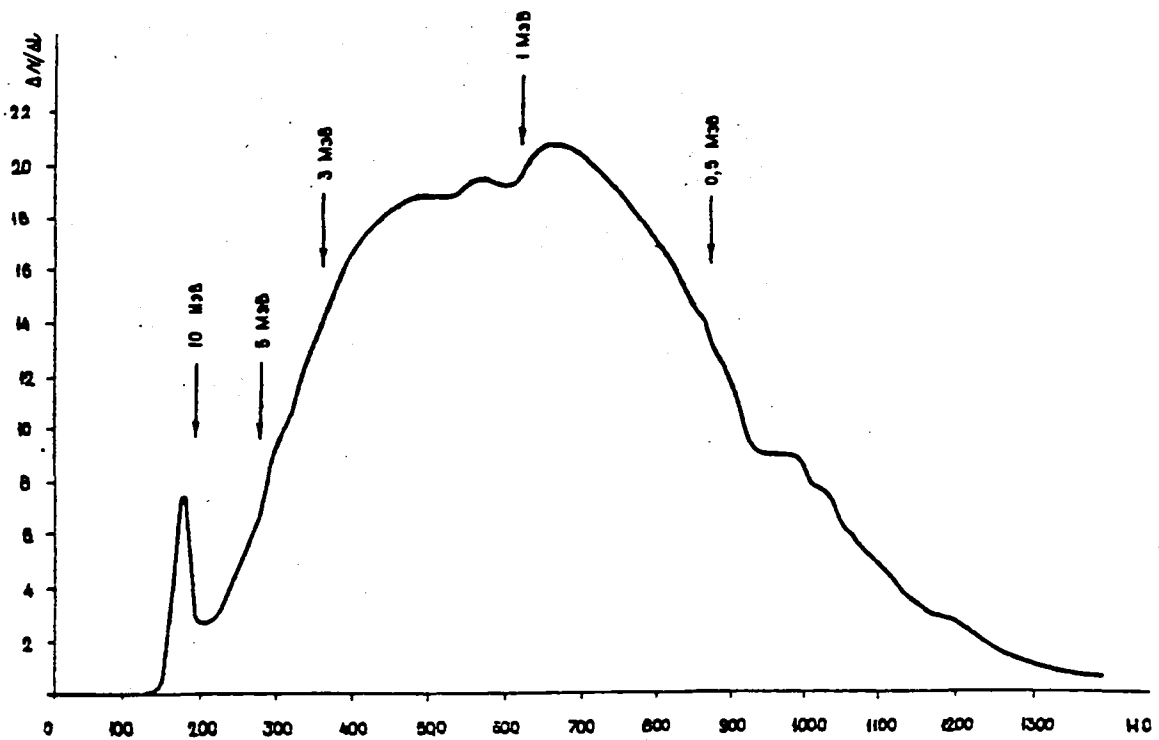


Fig. 22. Normalized measured spectrum of hemispherical sample of ^{238}U .

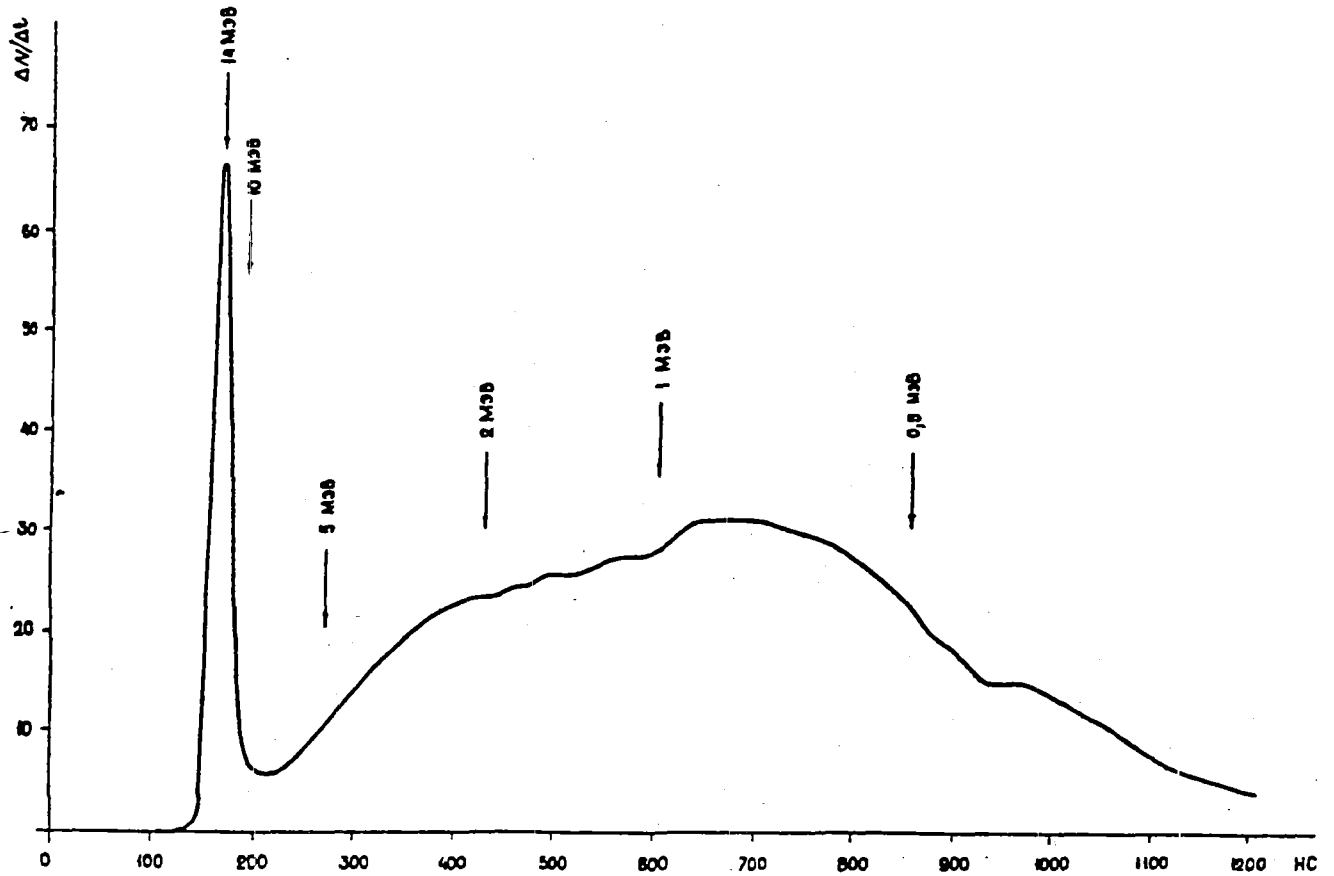


Fig. 23. Normalized measured spectrum of spherical sample of ^{238}U .

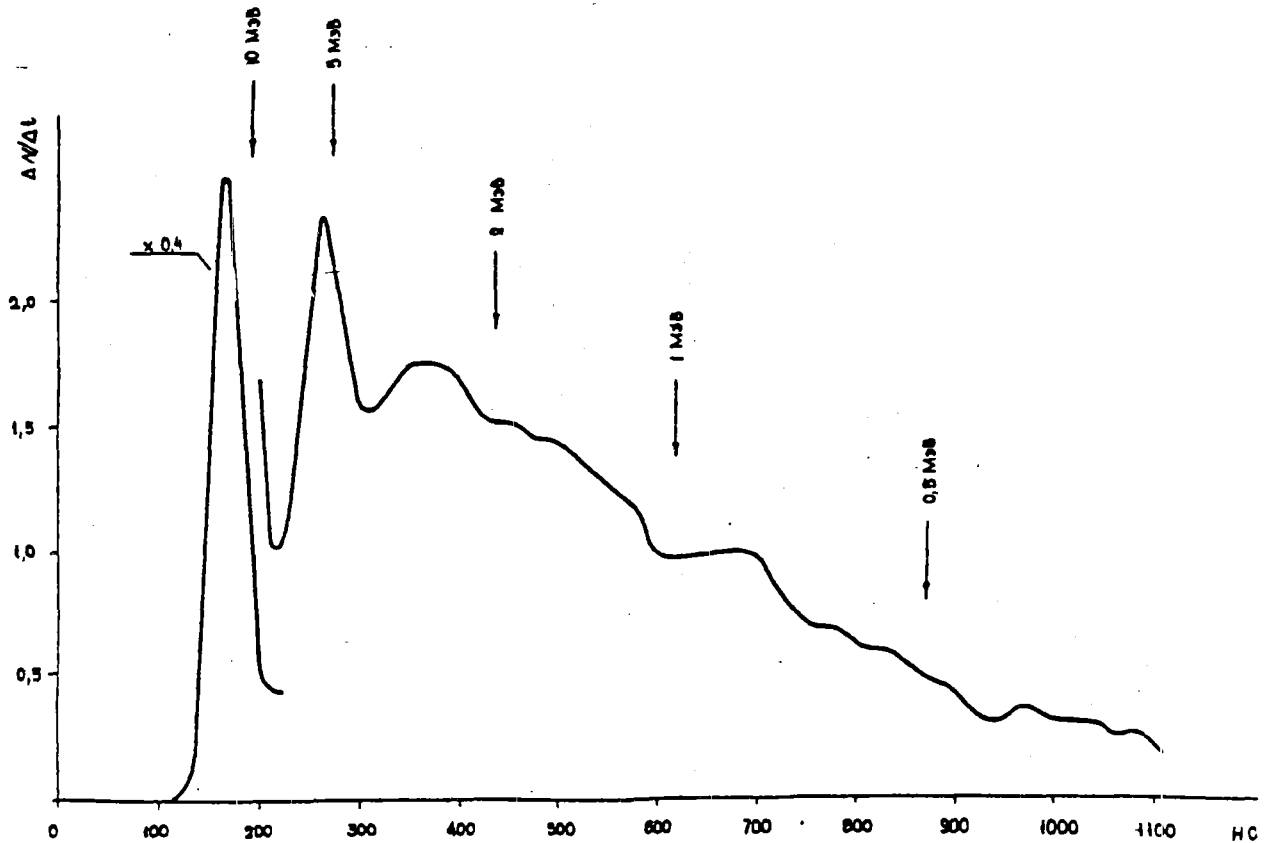


Fig. 24. Normalized measured spectrum of hemispherical sample of water

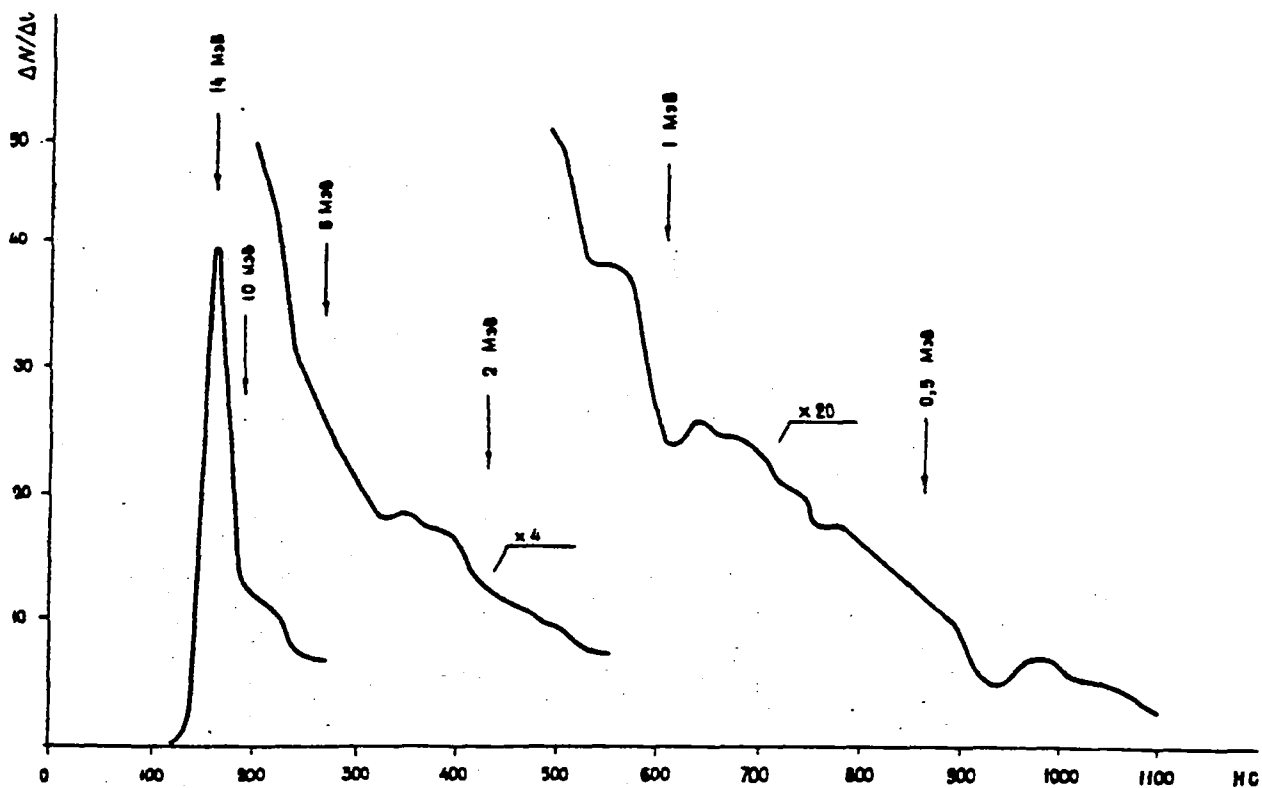


Fig. 25. Normalized measured spectrum of spherical sample of water.

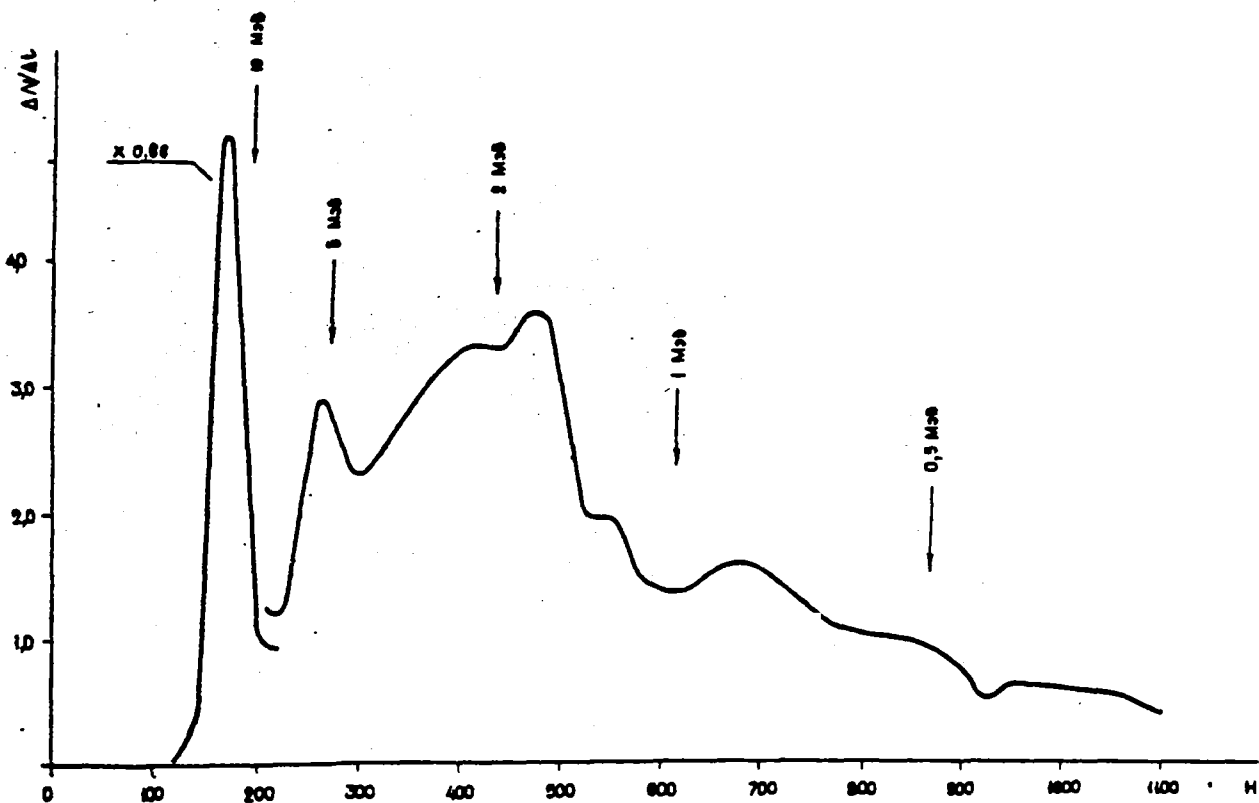


Fig. 26. Normalized measured spectrum of hemispherical sample of heavy water.

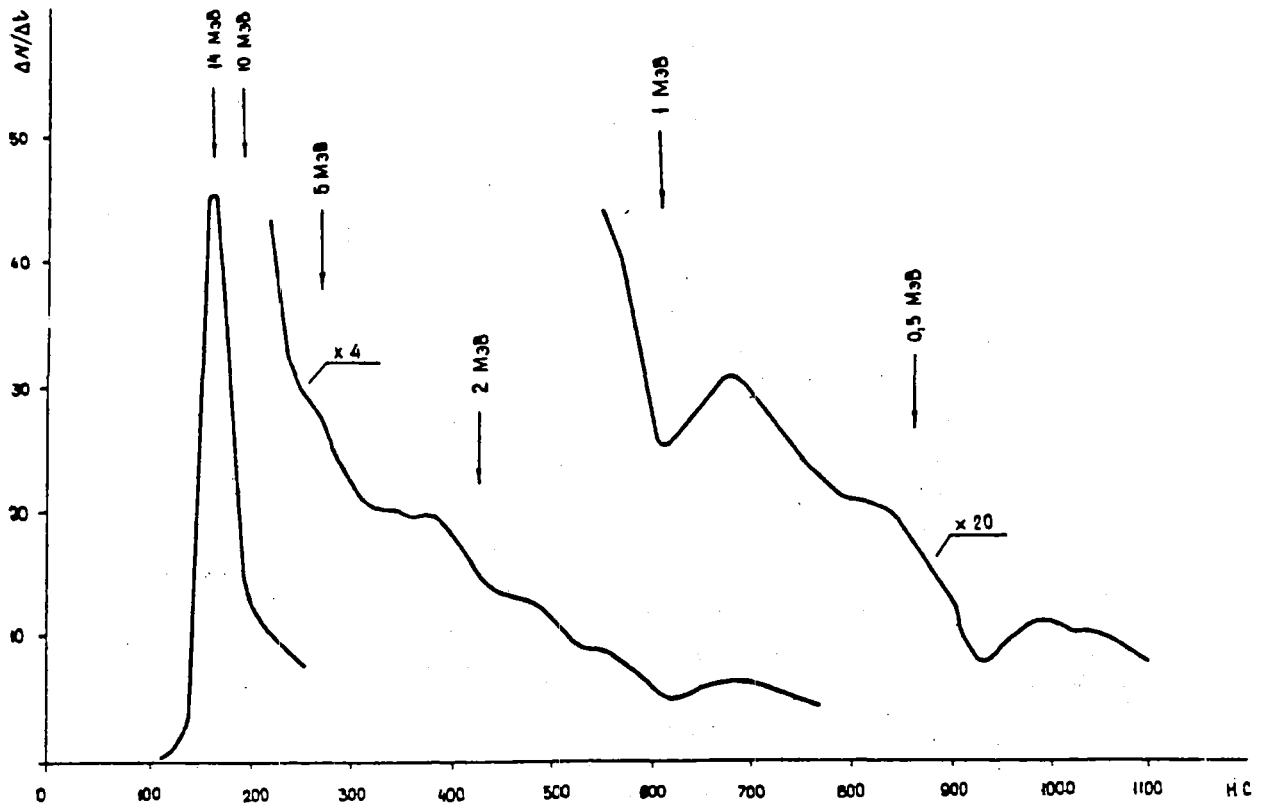


Fig. 27. Normalized measured spectrum of spherical sample of heavy water.

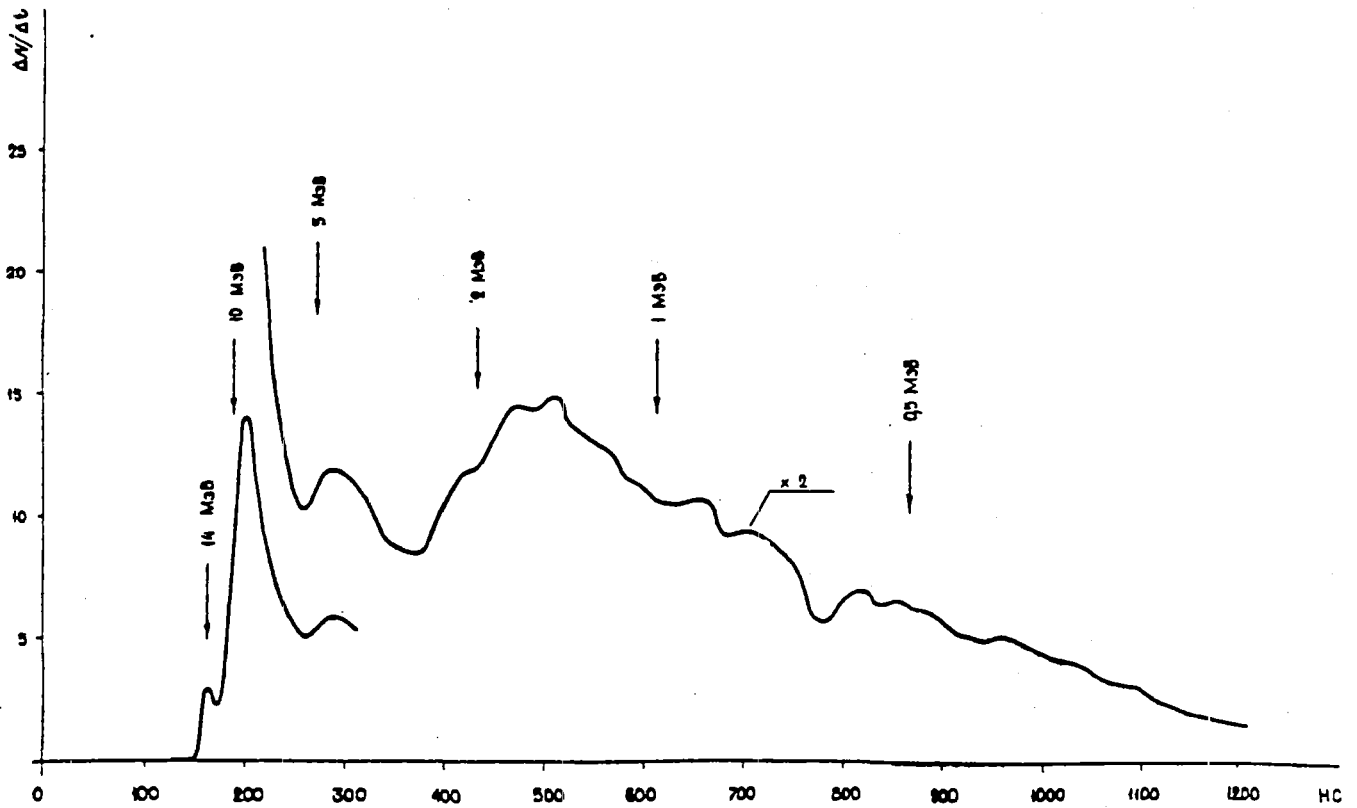


Fig. 28. Normalized measured spectrum of hemispherical sample of beryllium.

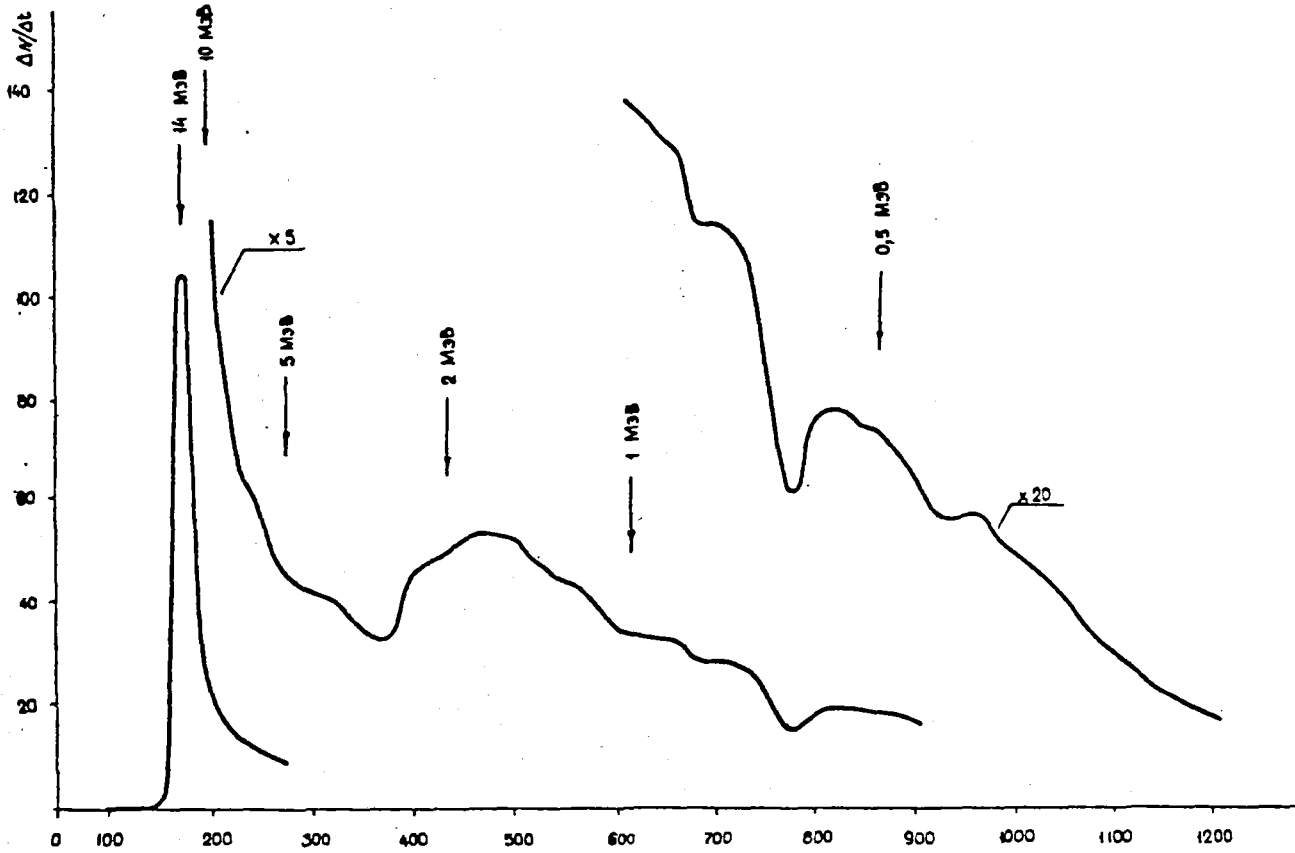


Fig. 29. Normalized measured spectrum of spherical sample of beryllium.

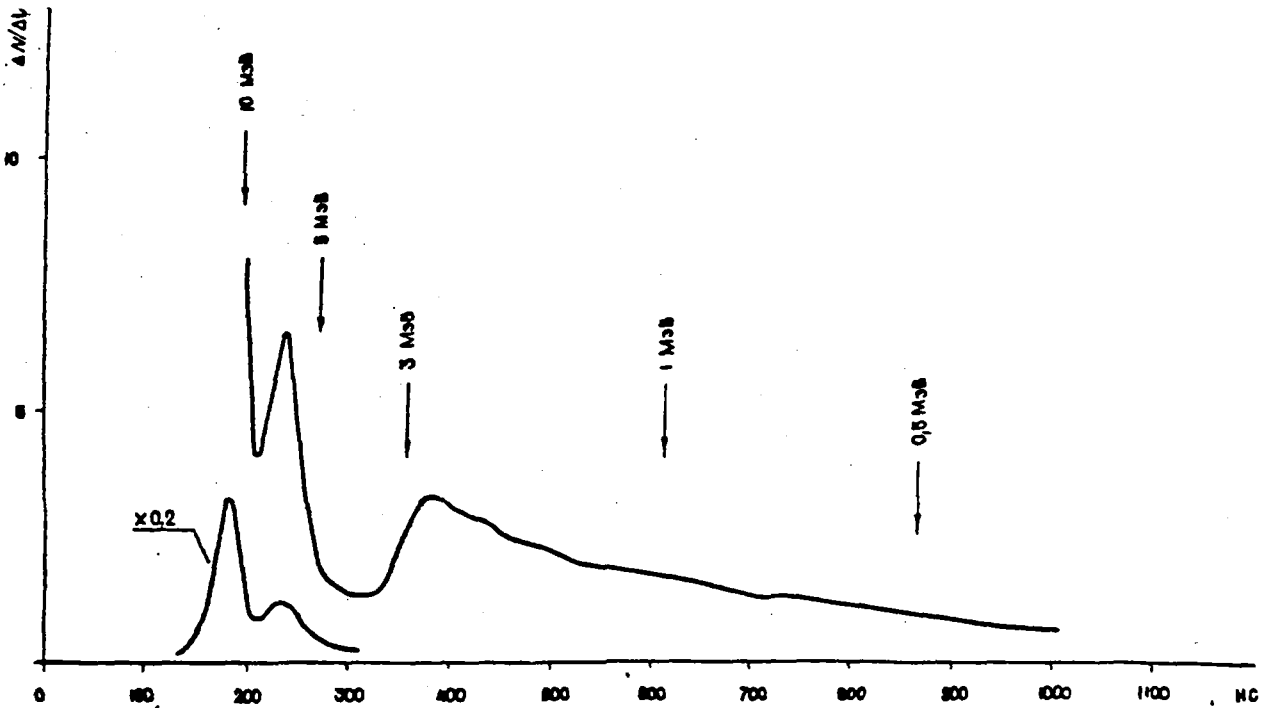


Fig. 30. Normalized measured spectrum of hemispherical sample of carbon.

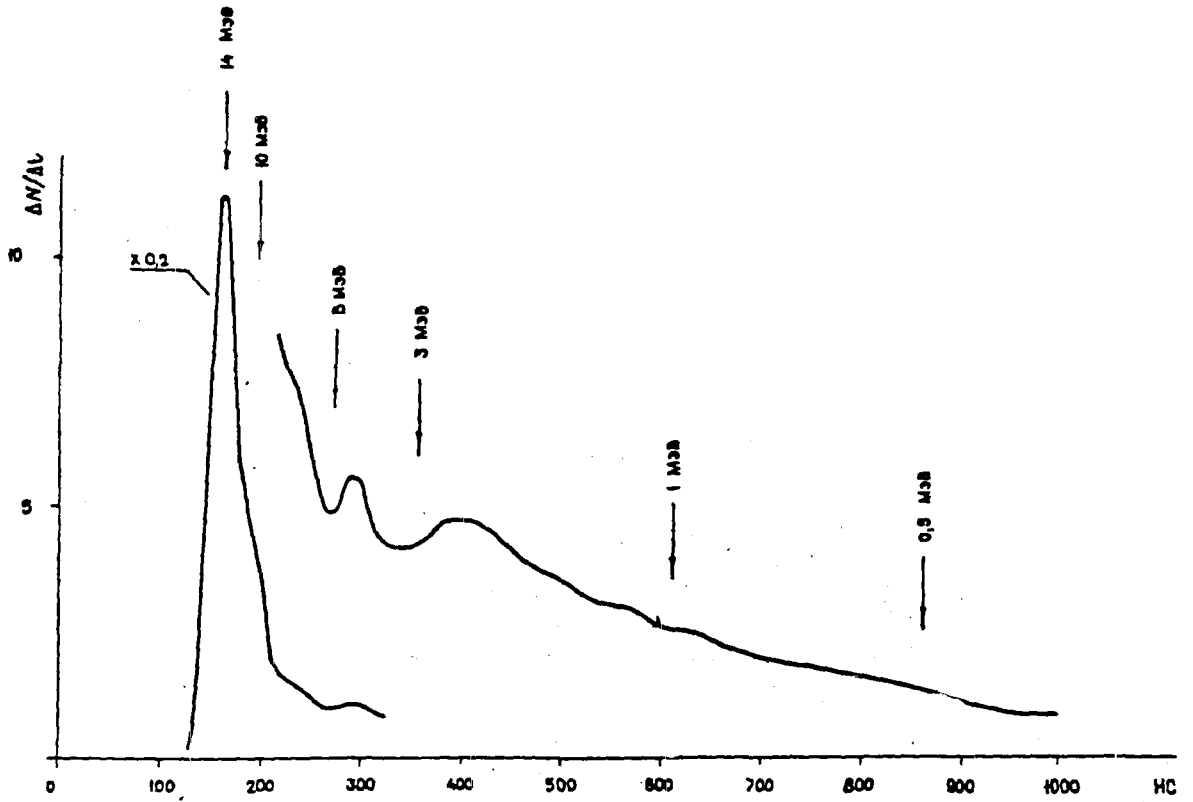


Fig. 31. Normalized measured spectrum of spherical sample of carbon.

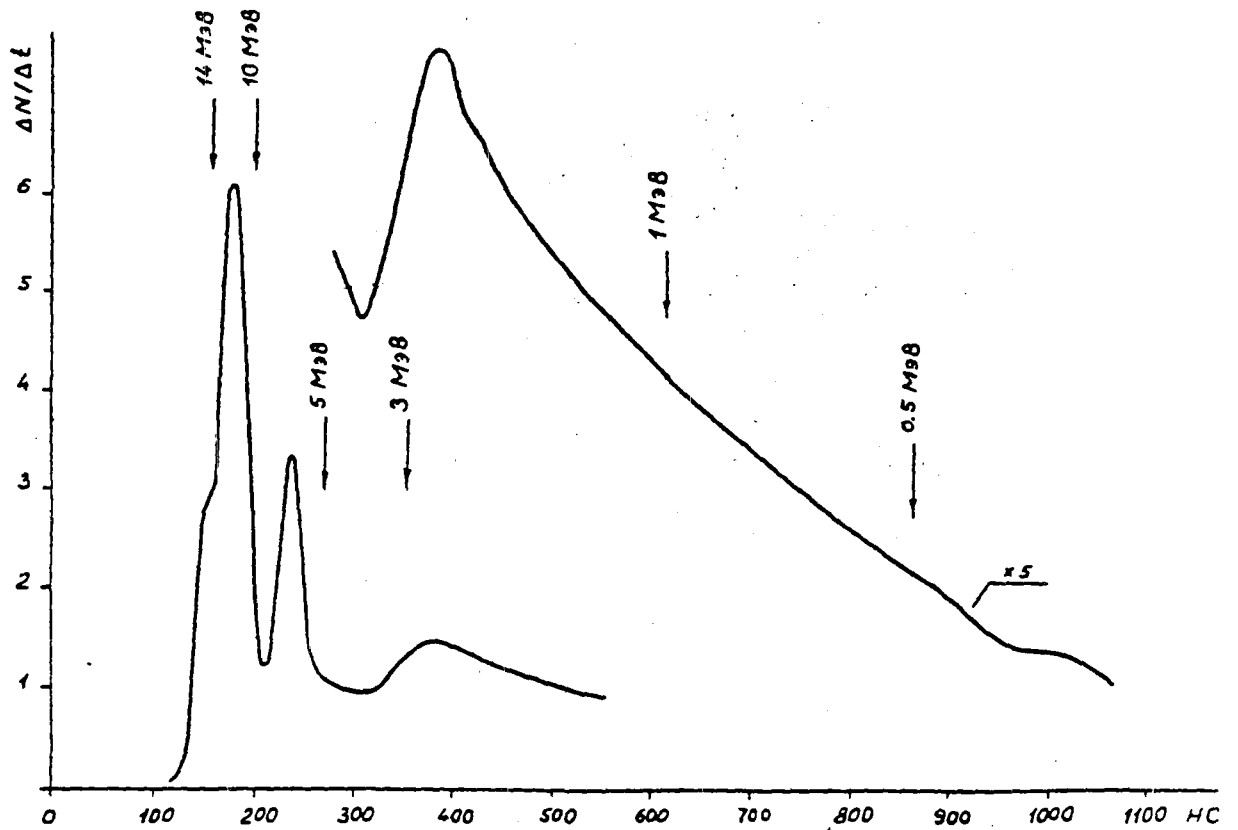


Fig. 32. Normalized measured spectrum of hemispherical sample of polyethylene.

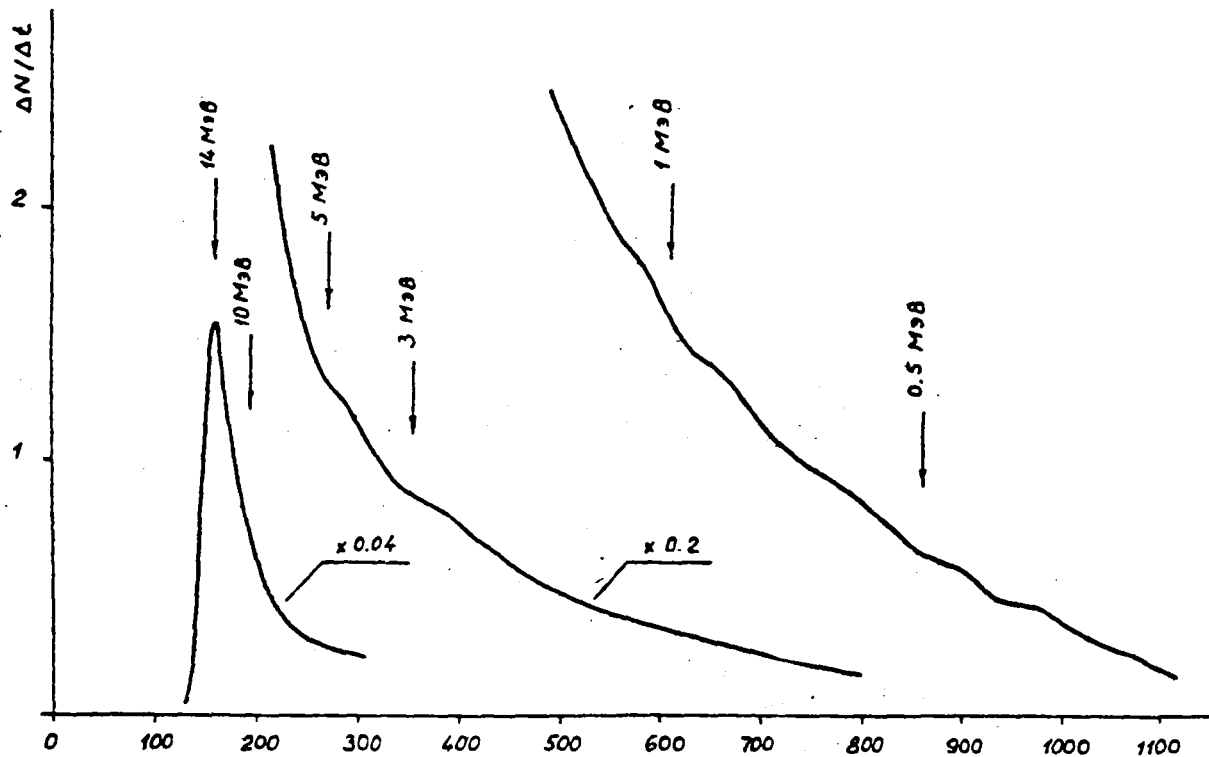


Fig. 33. Normalized measured spectrum of spherical sample of polyethylene.

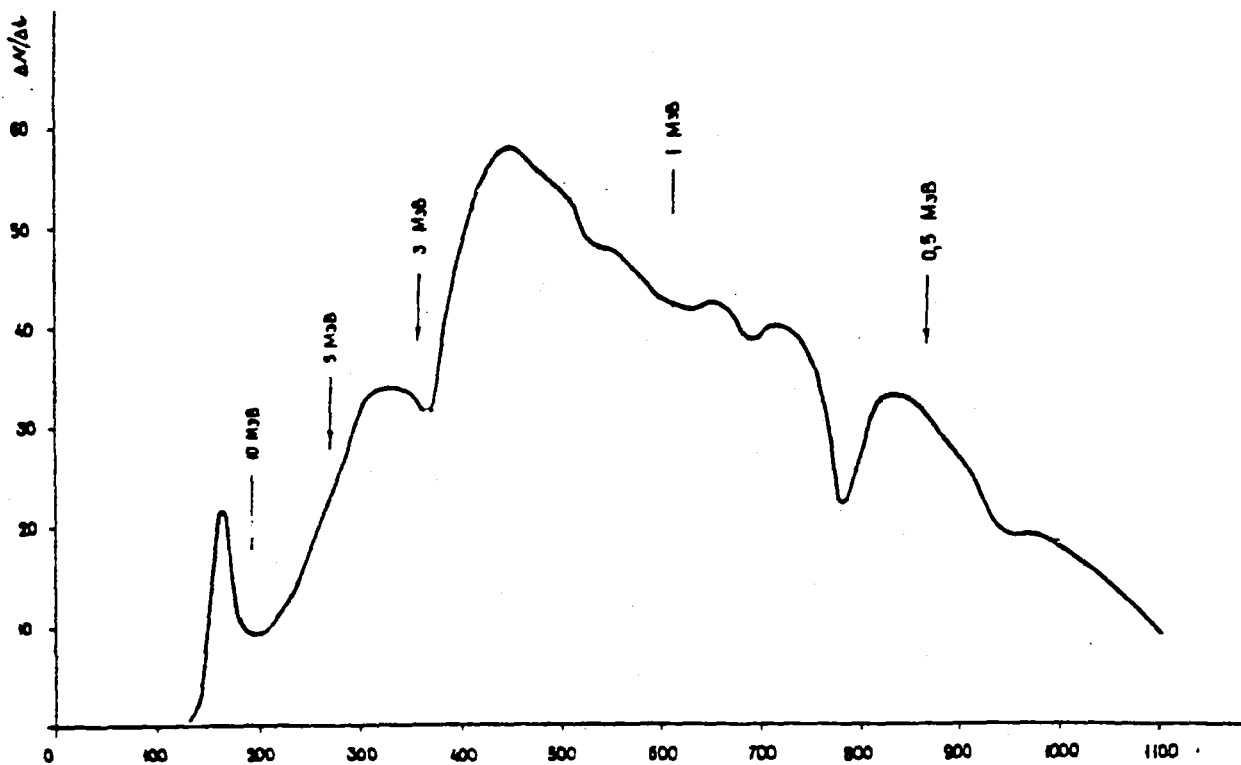


Fig. 34. Measured spectrum of hemispherical sample of ^{238}U which has passed through a 2 cm layer of beryllium.

REFERENCES

- [1] TRYKOV, L.A., Integral experiments for ionizing radiation transfer, Ehenergoizdat, Moscow (1985) [in Russian]
- [2] VASIL'EV, A.P., KANDIEV, YA.Z., KUROPATENKO, EH.S., "Measurements and calculations of 14 Mev neutron scattering on spherical samples of Pb" in: Collected Neutron Physics Reports, Kiev, (1987) [in Russian].
- [3] VASIL'EV, A.P., LYUTOV, V.D., AND KANDIEV, YA.Z., Verification of the neutron constants of ^{238}U , Be, CH_2 and Pb using the results of measurements on spherical samples, VNIITF (All-Union Scientific Research Institute Industrial Physics), (1989) [in Russian].
- [4] HANSEN, L.E., WONG, C., KOMOTO, T., AND ANDERSEN, J.D., Nucl.Sci. Eng. 60 (1976) 5.
- [5] STELTRS, M.L., ANDERSON, J.D., HANSEN, L.F., PLECHATY, E.F., AND WONG, C., Nucl. Sci. Eng. 46 (1971) 53.
- [6] HANSEN, L.F., ANDERSON, J.D., BROWN, P.S., HOWERTON, R.J., et al., Nucl. Sci. Eng. 51 (1973) 278.
- [7] DEVKIN, B.V., ZHURAVLEV, B.V., KOBOZEV, M.G., LYCHAGIN, A.A. et al., Voprosy Atomnoj Nauki I Tekhniki. Ser. Yadernye Konstanty, Vol.2 (1990) 5 [in Russian].
- [8] HANSEN, L.F., et al., Nucl. Sci. Eng. 92 (1986) 382.
- [9] YANAGI, Y., TAKAHASHI, A., Rep. A-84-02, Osaka (1984).
- [10] WONG, C., et al., Proc. Int. Conf. on Neutron Cross Sections, Washington, D.C. (1975) 704.
- [11] HANSEN, L.F., et al., Nucl. Sci. Eng. 72 (1979) 35.
- [12] ANDROSENKO, A.A. et al., International Conference on Neutron Physics, Kiev (1987) 194 [in Russian].

Submitted for publication 5 April 1991